CRYSTAL GROWTH AND INVESTIGATIONS ON THE EFFECTS OF HYDROGEN DOPING OF VO_2

A THESIS SUBMITTED TO

THE GRADUATE SCHOOL OF ENGINEERING AND SCIENCE

OF BILKENT UNIVERSITY

IN PARTIAL FULFILLMENT OF THE REQUIREMENTS FOR

THE DEGREE OF

MASTER OF SCIENCE

IN

MATERIALS SCIENCE AND NANOTECHNOLOGY

By

Koray Yavuz

March 2019

Crystal Growth and investigations on the effects of Hydrogen Doping of VO_2

By Koray Yavuz

March 2019

We certify that we have read this thesis and that in our opinion it is fully adequate, in scope and in quality, as a thesis for the degree of Master of Science.

Talip Serkan Kasırga(Advisor)

Aykut Erbaş

Abdullah Ceylan

Approved for the Graduate School of Engineering and Science:

Ezhan Karaşan
Director of the Graduate School

ABSTRACT

CRYSTAL GROWTH AND INVESTIGATIONS ON THE EFFECTS OF HYDROGEN DOPING OF VO_2

Koray Yavuz
M.S. in Materials Science and Nanotechnology
Advisor: Talip Serkan Kasırga
March 2019

Vanadium Dioxide(VO_2) has been studied extensively for its interesting electronic structure that allows it to go through Metal-Insulator Transition(MIT) at 65 °C. The nature of this phenomena is not entirely clear and more research is needed to firmly establish the science behind it and to realize possible applications; such as ultra-fast electrical and optical switching, sensor devices and Mott-Field Effect Transistors. One of the important experiments to understand the electronic structure of a material is Hall-effect measurements but due to acicular (needle like) nature of VO_2 crystals, this subject is only studied either on millimeter sized samples which are not suitable for many device applications or on poly crystalline thin films that are under non-uniform stress due to the substrate effects which gives unsatisfactory results when performing experiments. This thesis suggest a new method of chemical vapour deposition(CVD) growth for low aspect ratio VO_2 crystals that have lengths between 50-100 μm and thicknesses between 40-170 nm. These crystals can be mechanically removed from the substrate and transferred to use in different applications such as Hall-effect measurements or Transmission Electron Microscope(TEM) studies. Additionaly this work shows some aspects of the surface chemistry of the widely used Silica, Si, quartz and Sapphire substrates; relating with the control of oxygen saturation on the surface. Another VO_2 growth method for c-plane sapphire that leads to considerably more crystal yield is shown.

Hydrogenation of the VO_2 crystals suppresses the MIT so understanding this phenomena might help us better understand the effects lying behind the transition. To study this phenomena a crystal is doped only from half by blocking the passage of hydrogen to other half so the interplay between the insulating phase and hydrogenated conductive phase can be observed. As the analysis tool, TEM is used on this sample. Using a two-terminal device of a VO_2 crystal, the effects

of hydrogenation on the electronic properties have also been studied.

Overall this thesis introduces a new method for CVD growth of VO_2 which is used in various applications such as Hall-effect experiments, two terminal devices and TEM studies. To control the growth process the interplay between oxygen and surface chemistry of sapphire, silica, Si and quartz substrates have been investigated. With these studies a better understanding of the mechanics of growth is intended.

Keywords: Vanadium dioxide, Crystal Growth, Strongly Correlated Materials, Metal-Insulator Transition, Hall-effect.

ÖZET

VO_2 KRISTAL BÜYÜTMESI VE HIDROJEN ILE KATKILANMASININ ÜZERINE INCELEMELER

Koray Yavuz
Malzeme bilimi ve Nanoteknoloji, Yüksek Lisans
Tez Danışmanı: Talip Serkan Kasırga
March 2019

Vanadyum Dioksit(VO_2), 65 °C'da metal-yalıtkan faz geçişi gösteren güçlü etkileşimli bir materyaldir. Bu faz geçişi VO_2'nin önemli elektronik özelliklerinden kaynaklanmaktadır ama bu özelliklerin doğası kesin bir biçimde bilinmemektedir. Faz geçişinin arkasındaki fiziksel nedenler daha iyi bilinebilirse; ultra-hızlı elektriksel ve optik anahtarlama, sensör ve Mott-alan etkili transistör uygulamalarının hayata geçirilmesine katkı sağlanmış olur. Elektronik özellikleri anlamadaki önemli deneylerden biri Hall efekti deneyidir ama VO_2'nin asiküler(iğnemsi) doğası nedeniyle bu deney sadece ya milimetre boyundaki aygıt yapımı için uygun olmayan örneklerde ya da düzensiz strese sahip polikristal ince filmlerde çalışılmıştır ama bu örneklerden alınan ölçümler tatmin edici değildir. Bu tezde 50-100 μm arası ve 50-170 nm kalınlığında düşük en-boy oranlı VO_2 kristalleri üretmek için yeni bir Kimyasal Buhar Biriktirme kristal büyütmesi metodu sunmaktadır. Elde edilen kristaller mekanik olarak büyütme alttaşından alınabilmekte ve Hall etkisi ölçümleri ya da Geçirimli Elektron Mikroskopu çalışmaları için transfer edilebilinmektedir. Ek olarak yaygın olarak kullanılan silika, silikon, kuartz ve safir alttaşları için olan yüzey kimyası ve oksijen satürasyonu ile ilgili bazı hususlar gösterilmiştir. Safir c-düzlemindeki VO_2 büyütmesi için önemli ölçüde randıman veren bir metot da geliştirilmiştir.

VO_2 kristallerinin hidrojen ile katkılanması metal-yalıtkan faz geçişini bastırır, bu olayın anlaşılması faz geçişinin arkasında yer alan etkileri anlamamıza yardımcı olabilir. Yalıtkan faz ile hidrojen ile katkılanmış iletken faz arasındaki ilişkiyi incelemek için bir tekil kristal VO_2 kirişi yalnızca yarısından hidrojenle katkılanmıştır. Analiz için Geçirmeli Elektron Mikroskobu kullanılmıştır. İki uçlu bir VO_2 aygıtı kullanılarakda hidrojen katkılanmasının kristalin elektronik özellikleri üstündeki etkisi incelenmiştir.

Özetle bu tez Hall-etkisi incelemeleri, iki-uçlu aygıt yapımı ya da Geçirmeli Elektron Mikroskopu çalışmalarında kullanılması amacıyla 50-100 μm boyutlarında ve 75-170 nm kalınlığında düşük en-boy oranlı tekil kristal VO_2'nin Kimyasal Buhar Biriktirme'sinde yeni bir kristal büyütme yöntemini sunmaktadır. Büyütme sürecini yönetmek için silika, silikon, kuartz ve safir alttaşlarındaki yüzey kimyası ve oksijen arasındaki ilişki araştırılmıştır. Bu metotlarla birlikte VO_2'nin kristal büyütme mekanizmasının daha iyi anlaşılması hedeflenmektedir.

Anahtar sözcükler: Vanadyum dioksit, Kristal Büyütmesi, Güçlü Etkileşimli Malzemeler, Metal-Yalıtkan Faz Geçişi, Hall-efekti.

Acknowledgement

I would like to thank my advisor Dr. T. Serkan Kasırga for his guidance during my study. I would like to thank to all scmlab members, old and new, whom I've learned and received help whenever needed; especially Engincan Sürmeli and Mustafa Fadlelmula. I would like to thank my parents Kenan Yavuz and Yurdagül Yavuz for their unconditional love and support which is one of the biggest reasons I am able to pursue my career goals. I would also like to thank my brother Kaan Yavuz for his endless support and care. I would like to thank to thank my friends from my old and new dorm, Hüsna, Dilara, Hatice, Nurcan, İhsan, Denizcan, Gamze, Fulya, Nermin abla, Mustafa Kahraman and many others with whom I've had very enjoyable time together and of course dining. Finally, I would especially like to thank Uğur Teğin, Onur Çakıroğlu, Abdüllatif Önen, Begün Erbaba, Assel Amirzhanova, Eliza Sopubekova, Ulviyya Quliyeva and Özge Beğli, for their great friendship in which I've found immense amount of joy.

Contents

List of Figures

Chapter 1

Introduction

In general, repulsive electron-electron interactions can be overlooked when the properties of the materials are determined via theoretical calculations. The electrical, mechanical and thermal properties of silicon, diamond, graphene and many other materials, are not strongly affected by the electron-electron interactions. However this is not the case for strongly correlated materials[6]. Many interesting phenomena such as colossal magnetoresistance where small changes in magnetic field causing huge variance in resistance, high-temperature superconductivity or metal-insulator transition can be caused by systems where electrons are strongly correlated[7]. However these strong interactions also make the strongly correlated systems hard to study, many of the controlled theoretical methods don't work in such systems. Widely used methods that can predict electronic behaviour such as Hartree-Fock approximation, (k.p) expansion and many others require electron-electron repulsion to be comparatively weaker to kinetic energy of electrons. The d-electron and f-electron systems provide interactions where these electron-electron repulsion effects are comparable to the kinetic energy of the electron like in vanadium dioxide, where vanadium ions each have a single unpaired d electron[6]. As we we will dwell in next chapters, experiments are also challenging in these materials. Understanding the strongly correlated systems can allow us to predict and manipulate their properties, but first the techniques and methods used in strongly correlated materials research

should be improved. In the next chapters we will consider the properties of a strongly correlated material, vanadium dioxide(VO_2) and the issues relating to its research.

1.0.1 Vanadium Dioxide

Vanadium Dioxide (VO_2) is a strongly correlated material that goes through metal-insulator transition (MIT) with critical temperature at $T_c = 67\ ^\circ$C[8][9][10]. It is an n-type semiconductor with monoclinic structure below T_c[1]. Above the T_c it becomes a poor metal with a rutile-tetragonal structure. In the literature there are different values presented as the band-gap of the monoclinic (M1) phase, 0.3 eV[11], 0.4 eV[12] and 0.7 eV[1]. In the rutile phase of VO_2, the cubic component of the $V^{4+}(3d^1)$ ion octahedral sites are first split into twofold-degenerate e_g levels and threefold-degenerate t_{2g}[13]. t_{2g} further splits into $d_\parallel$ and π^* levels which are the lowest energy levels near the fermi level[1]. The band gap between the bottom of π^* conduction band and the top of the $d_\parallel$ valence band is measured to be 0.7 eV by ultraviolet photoemission spectroscopy and ultraviolet reflectance spectra measurements. The schematic of the band structure can be seen in figure 1.1.

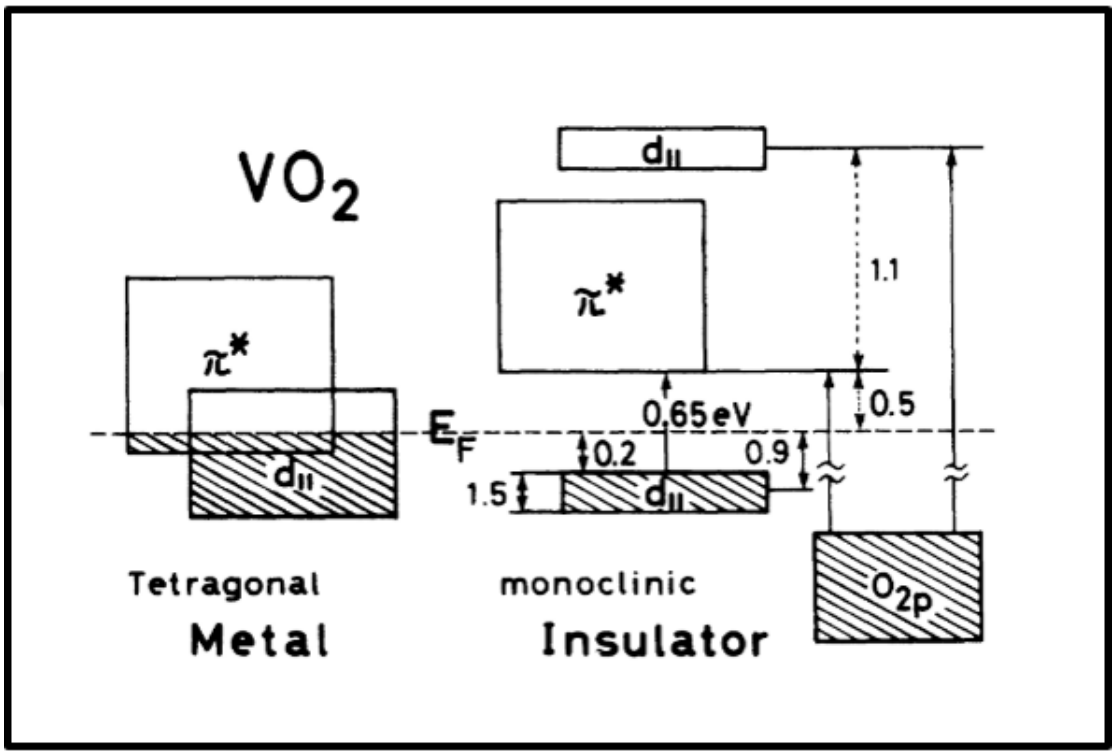

Figure 1.1: Schematic band structure of the 3d bands around the Fermi level of VO_2. The energy of 0.2 eV is obtained by ultraviolet photoemission spectroscopy, the energies of 0.5 and 1.1 eV are obtained by ultraviolet reflectance spectra and 0.65 eV is obtained from infrared absorption spectra[1]. Reprinted figure with permission from [Shin, Shik, et al. "Vacuum-ultraviolet reflectance and photoemission study of the metal-insulator phase transitions in VO 2, V 6 O 13, and V 2 O 3." Physical Review B 41.8 (1990): 4993.] Copyright (2019) by the American Physical Society.

1.0.2 Structure of Vanadium Dioxide

VO_2 have various structural phases including VO_2(M1), VO_2(M2), VO_2(T), VO_2(R), VO_2(A), VO_2(B). The structure that has MIT at $T_c = 67$ °C is VO_2(R) which is the focus of this study. When using CVD growth method using V_2O_5 as precursor, at growth temperatures VO_2(R) phase is more favorable, so in regular CVD growth the rutile phase is grown which turns to monoclinic phase M1 at

room temperature [14]. The monoclinic M2 and Triclinic T phases become stable with the increasing tensile stress, with T phase being in between the M1 and M2 phases however transformations from M1 to M2 and from M1 to T and then to M2 are both possible [15]. Same thing with M1 and M2 phases which both can turn into rutile phase after 67 °C, and they can be found coexisting close to MIT temperature [16]. The M2 and T phases are not stable phases, but can be stabilized with stress[15][17][18] or doping[19][20]. Thus when talking about pure VO_2 with negligible stress we focus on the M1 and R structures of VO_2. The rutile structure (Tetragonal phase) has space group $P4_2/mnm$ with lattice constants a=4.5540 Å and b = 2.8557 Å at 400 $°K$. The M1 phase has a monoclinic cell with space group $P2_1/c$ and $\beta = 122.61°$ and a = 5.7529 Å, b = 4.5263 Å, c = 5.3825 Å at room temperature [21]. In M1 phase half of the V chains are twisted with no pair and the other half is not twisted and paired; as it goes to transition to rutile phase these V chains get paired without twisting which is accompanied by a large spectral weight transfer due to changes in orbital occupations that leads to increased electron carrier density[22][23].

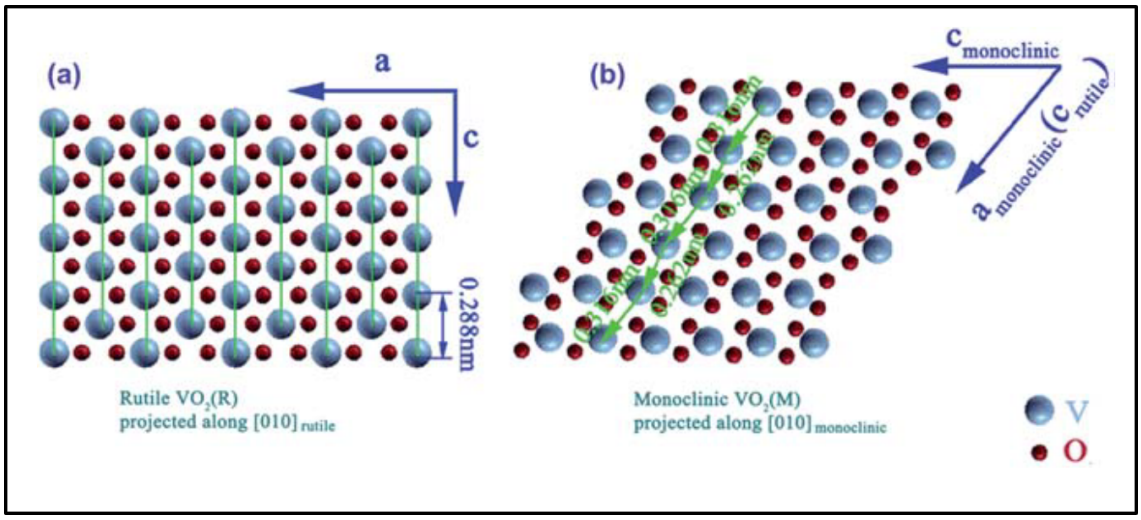

Figure 1.2: Monoclinic (M1) and Rutile (R) Structures of VO_2

1.0.3 Nature of Metal-Insulator Transition

The nature of the metal-insulator transition is not fully understood, one of the reasons for it is that the transition showing elements from both the Peierls and the Mott transitions, and it can be said the transition is an interesting Mott-Peierls transition[24]. However due to connectedness of two events, determining the main effect that starts the whole process is a challenge; is it the electron density change coming from Mott transition that alters the structure of the VO_2 crystal or Peierl's transition occurs before the electron density change? Another important question is, why and how these two events are entangled? To have insight on this topic we need to consider both transition cases, since VO_2 contains both events happening regardless of the time order.

Peierl's insulators refer to the materials that exhibit insulating behaviour due to static lattice deformations and mott insulators are due to electron-electron interactions. While the periodic potential of the crystal affects the electrons' motion, the presence of electron may also bend the lattice due to coulomb force between the ions and the electron. If the energy gain by the electrons is large enough for the lattice deformation, the new periodic potential may lead to a metal-insulator transition [25]. This is called a Peierls transition and it is a type of thermodynamic phase transition. VO_2 shows many features of Peierl's transition, using soft-x-ray absorption spectroscopy M.W. Haverkort et al. showed that the V $3d$ orbital occupation changes in a way that the charge fluctuations and effective bandwidths are reduced and the system electronically more one dimensional which makes it susceptible to a Peierls-like transition[24]. There are some studies that claims this is the main event that needs to take place for the MIT, by using ultrafast spectroscopy techniques, A. Cavalleri et al. initiated the MIT in VO_2 by prompt hole photo-doping into the valence band of the insulating phase of VO_2 and they observed that the structure change came before the transition to conducting phase[8]. However claims to contrary also exist.

Mott transition considers a system where electron-electron interaction creates a gap in the spectrum for single charge excitations, this strong correlation leads

to a para-magnetic Mott-Hubbard insulator where local magnetic moments in the crystal don't display long-range order [25]. While the electron gas screens the positive charge on the donors(or ions), the potential seen by a single electron becomes

$$V(r) = \frac{e^2}{\kappa r} exp(-qr)$$

where κ is the dielectric constant of the material and q is the Thomas-Fermi screening constant[26]. The q value depends on electron density and if it is large enough there is no bound state for electrons so it shows metallic behaviour; however at a critical value of low electron density bound states start to occur as well as a transition from metal to insulator[26]. The electron density in the valence orbitals may increase with regular temperature increase or another event which can make the crystal reach the critical electron density value. When we are considering the case of Vanadium Oxides we should consider a case where the attractive force between the positively charged centers and electrons are very small, so some of the electrons might be very close to escape from the ion centers close to room temperature. If a pair of V^{4+} and V^{+2} ions are formed they can both form polarons and that the energy released by these polarons may be enough for the energy required to form a pair of carriers in VO_2 lattice. So Mott's hypothesis on the subject of vanadium oxides is that the metallic phase of vanadium oxides such as V_2O_3 or VO_2 is not really metallic and the electron density required by the Mott-transition comes from nondegenerate gas of small carriers that are formed by the polarons of V^{4+} and V^{+2} ions[27]. G. Stefanovich et al. supported the Mott transition picture with experiments that involves electron injection into the VO_2 directly so that the q value would be increased without the help of temperature, and they were able to observe MIT at temperature below the T_c[28]. Hall-Effect measurements of Ruzmetov et al. also can be used as an evidence showing that the transition comes from the electron density increase[29]. The experiments of Hyun-Tak Kim and colleauges claim that they could onserve a MIT without the structural change using their micro-Raman system[30], and femtosecond pump-probe measurements[22], supporting this stance.

The MIT of VO_2 can lend itself to some promising switching and sensor aplications which use different aspects of VO_2. When compared to other metal

oxides, VO_2 goes through MIT closer to the room temperature, at 67 °C, and can be modified to be doped to lower the temperature of MIT further[31][32] which increases its stability and lowers the energy consumption[33]. There are applications in the areas of optical switching where the fast response rate to photo excitation is used. As the VO_2 nanoparticles become metallic, they start to have surface-plasmon resonance which exhibits ultrafast enhancement of optical absorbtion near telecommunication wavelengths[34]. This plasmon resonance can be also controlled by the shape of the VO_2 nanoparticles.

VO_2 can also be used for smart window coatings, which are coatings that alter light transmission properties; VO_2 can change its infrared transmittance according to temperature of the environment[35]. Th Jiadong Zhou et al. observed that the scattering properties can be altered by controlling the size of the VO_2 particles.

Another area of application is using VO_2 for fabricating sensors. One type is a VO_2 nanowire thermistor device that Strelcov et al. introduced that acts as a TES-like sensor which can detect the change in rate of heat transfer from the gas molecules in the environment, though it's not selective to gas type[36]. Another type of gas sensor is a selective type that uses the reversible doping of VO_2 with atomic hydrogen. This leads to stabilization of the metallic phase that is stable till 4.2 °K along with a significant increase in conductivity [37]. This can be used in very sensitive hydrogen sensing devices, and can even be used to detect other type of gases albeit with lower sensitivity [33]. The different phases of VO_2 can be also utilized for interesting stress-strain sensor that uses M1–M2 phase evolution of VO_2[38].

1.0.4 Hydrogen Doping of Vanadium Dioxide

The doping process involves the intercalation of the atomic hydrogen into VO_2 lattice from the c-plane of rutile phase and this changes the structure to O1 or O2 orthorombic phases[39]. The intercalation induces the lattice constant 'b' of rutile phase to increase[40], however how the hydrogen exactly diffuses in the

crystal is unknown due to challenge of observing the exact hydrogen content in any place[37]. We tried to tackle this problem using TEM techniques in which we used single crystal thin Nanobeams. More understanding in this area would supplement the research in both device making and hydrogen doping.

An important area for this type of study can be protonics. Fuel cells can convert chemical energy to the electrical energy directly, and a proton conductor can be an important part of it[41]. VO_2 can diffuse singular hydrogen atoms inside it but there are no applications yet. By showing control over crystal structure and control over this hydrogen diffusion, promising applications may be realized.

1.0.5 Problems that emerge in VO_2 Research

The ambiguity of the results in the VO_2 research can be partially explained by reasons such as different domain structures formed after MIT and non-uniform stress caused by the substrate, which alters the electronic properties of the material so that experiments give conflicting results [42]. When the crystal grows on a substrate at high temperatures, the stress occurs naturally at room temperature due to different coefficients of thermal expansion of the crystal and the substrate. Because of the MIT there is another source of stress occuring via the structural phase. As Wei et al. remarked in their 2009 paper, to have reproducable results in research and to use VO_2 as a component of an optical or electronic switching device; aforementioned issues should be resolved. One of the important topics for the research of the electronic system of VO_2 is hallbar measurements that can give valuable information on the nature of the transition and VO_2. Hall effect of thin VO_2 crystals in high magnetic field and also other electron-transport behaviors close and across the MIT are very important[29]. However Hall-effect measurements are complicated because of low hall-mobility, low-hall voltage and unusually high noise coming from hall contacts at insulating phase due to previously mentioned stress problem[29] [43].

For Hallbar measurements, the best results ideally would be taken from a VO_2 single crystal with a hall bar shape. However owing to its acicular nature

most of the VO_2 growth is focused on making rod shaped crystals[44],[45],[46]. Because of this, a method that produces large single crystal platelets is required. A thin crystal with low aspect ratio can be shaped to a desired Hall-bar shape and larger it is, easier it is to transfer and pattern it using lithography methods; so our project aims to find a growth technique that would produce crystals that are large enough to handle which is at least 20 μm length and 10 μm width with preferably low thickness, less than 150 nm. These single crystals may also give better and more precise results when using in other techniques such as raman systems or pump-probe measurements due to its large size being able to accommodate large laser spots. For example in the work of Martin R. Otto et al., they use ultrafast electron diffraction to determine the phase change of a 50-nm-thick polycrystalline VO_2 sample as it is photoexcited by a 35-fs 800-nm optical pump pulse[47]. Because of the polycrystalline film, many of the VO_2 grains don't go into phase change at the same time which gives imprecise results. The results can be a lot more precise with a stress-free large single crystal VO_2.

1.0.6 Outline

The first part of this thesis describes the new methods developed for the growing of VO_2 crystals that are required to use in Hall-effect and TEM measurements and VO_2 device making. This part involves the description of growth dynamics on 1 μm SiO_2, p-doped Si, c-plane sapphire and quartz substrates and how to manipulate the chemical potency and nucleation rate of the crystals in those substrates. with the method provided; control over crystal shape, thickness and length on 1 μm SiO_2 and c-plane sapphire substrates are presented.

The second part shows our work in TEM analysis of hydrogenated VO_2 single crystals. We show the point we reached in TEM devices; how to make them, challenges and what remains to be done. VO_2 crystals are doped only on one side in such a way that half of the crystal would be hydrogenated while other stays unhydrogenated and two zones are divided with a distinct line. Using Selected Area Electron Diffraction the lattice transformation caused by the hydrogen

doping is analysed.

The third part is about device making for the purposes of analyzing the effects of hydrogen doping on the electronic properties of VO_2. While the experiments weren't a success, the problems faced and the device making methodology is described.

Chapter 2

Crystal Growth of VO_2

Various growth techniques for VO_2 exist in the literature, such as magnetron sputtering, sol-gel, pulsed laser deposition(PLD) and chemical vapor deposition(CVD). PLD method involves ablating the sputter target which creates a plasma then deposits the target material onto the substrate. Magnetron sputtering utilizes magnetrons to confine a gaseous plasma on the surface of a sputter target which contains the material to be deposited. The confinement of plasma on the surface of the target increases the deposition rate with no damage done to substrate or growing film. Both PLD and magnetron sputtering are well established industrial techniques for deposition onto rigid and flexible substrates and they can produce a large area VO_2 thin film with good crystallinity[48]. Using reactive dc magnetron sputtering, Shu-Yu Li et al. showed that VO_2 thin film with 34nm thickness can be grown on glass substrates[48]. However the VO_2 thin films created by PLD method[49] and magnetron sputtering[48][50] are polycrystalline. Another disadvantage of this technique is that the stress coming from the substrate alters the properties of the crystal. In Dong-ping Zhang et al. work 84nm thick VO_2 thin film is deposited on soda-lime glass substrate using reactive dc magnetron sputtering; and the MIT temperature becomes approximately 50°C instead of 67°C of the stress free single crystal. The epitaxial films created by PLD on substrates such as sapphire[51] or TiO_2[52] face similar stress problems due to lattice mismatch which changes the MIT temperature and

alters properties such as electrical conductivity[51]. Another issue with epitaxy or other methods would be the complexity of actually removing the films from the surface and manipulating them. These issues make magnetron sputtering and PLD undesirable for our projects.

The sol-gel method can also provide large area thin films. The sol-gel method involves creating a solution consisting a solvent and chemical precursor that can be metal alxoxide, metal salt or a molecular precursor which is turned into a gel by condensation. The resulting gel is spin coated or dip coated on substrate then it is annealed at approximately 600°C to crystallize VO_2[53]. The sol-gel technique is relatively simple and it doesn't require complex equipment which makes it low cost, unlike magnetron sputtering and PLD which requires dedicated equipment. However sol-gel methods suffer from the same problem of creating polycrystalline film[54][55].

We chose low pressure CVD growth to produce thin, large area VO_2 single crystals. One growth method developed by Hongkun Park's group produces single crystal VO_2 nanowires with rectangular cross sections on substrates such as Si_3N_4 and SiO_2[56]. They used bulk VO_2 powder as precursor and went up to 900-1100 °C to initiate the deposition under 12-13 $Torr$ pressure; the grown crystals had thickness at 60($\pm$30)nm and lengths up to 10 μm. Another single crystal VO_2 growth method developed by Baik et al. produces 140nm thick crystals with lengths around 20-150μm on substrates of single crystal Si wafers covered with 200nm SiO_2 layer[57]. The growth was done under atmospheric pressure using VO_2 powder as precursor and the growth temperature was in the range of 550-650 °C.

Advantages of these methods are the simplicity of the methods and availability of required equipments in a regular lab environment. Also these methods provide single crystals that can be removed from the surface for further manipulation[36]. However the crystals have a preference in growth direction of (001) of rutile phase, which leads to wire like morphology[56][57]. Because our projects require thin and low aspect ratio crystals that can be patterned and manipulated easily, these methods were not satisfactory. To produce such crystals, the mechanics of growth

should be understood.

2.0.1 Mechanics of crystal growth of VO_2

Since the melting point of the bulk VO_2 is 1782 °C[58] it is not the optimal precursor to use. As Strelcov et al. demonstrated that it is the V_2O_5 impurities present in VO_2 that evaporates and causes the VO_2 growth[2]. Due to this reason we used V_2O_5 as precursor. Vanadium-Oxide system is a complex one due to various oxidation states the vanadium atom can take, +2, +3, +4, and +5, this results with many components available including V_2O_5, V_6O_{13} and VO_2. The growth model suggested by Strelcov et al. for CVD growth on SiO_2 substrate is that as the V_2O_5 precursor melts around 680 °C it makes a 'fuel dome' melt which first turns to V_6O_{13} by losing oxygen then turns to VO_2 which is stable for the conditions that we use, 10^{-2} mbar pressure and between 700-1000 °C [2]. Strelcov et al. state that the fuel domes create VO_2 nucleations that begins to turn the liquid melt to a crystal. The melt wets the formed crystal along its sides to the tip and due to preference of VO_2 to grow mainly on the c-axis of the rutile phase, the final crystal shape becomes rod-like if there is no interaction with other fuel domes. This process of the precursor V_2O_5 turning into VO_2 is shown in Figure-2.1.

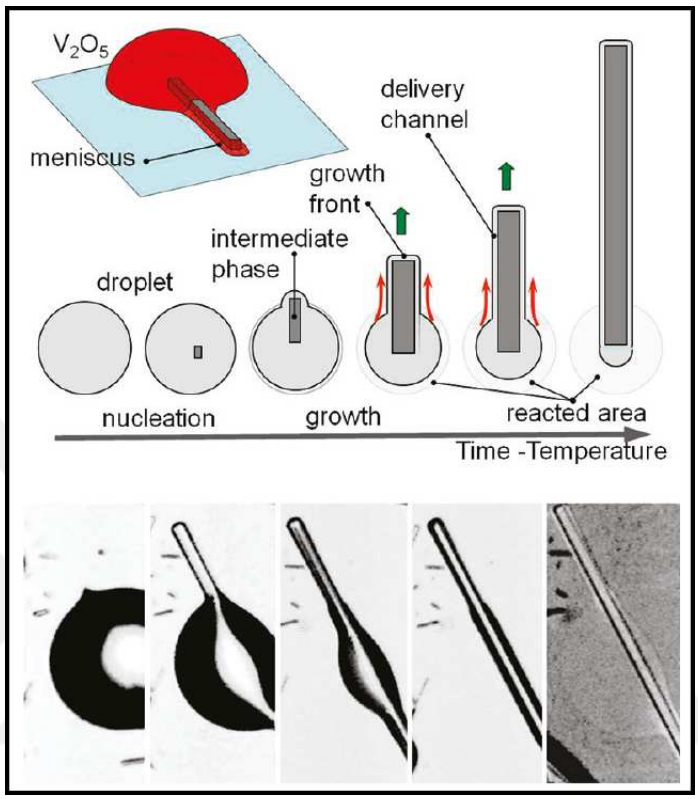

Figure 2.1: VO_2 crystal forming from a fuel dome. Reprinted with permission from (E. Strelcov, A. V. Davydov, U. Lanke, C. Watts, and A. Kolmakov, "In situ monitoring of the growth, intermediate phase transformations and templating of single crystal vo2 nanowires and nanoplatelets," ACS Nano, vol. 5, no. 4, pp. 3373–3384, 2011). Copyright (2011) American Chemical Society[2].

Strelcov et al.'s article provides a very useful analysis of the growth features, however it does not provide enough information to make very thin crystals with low aspect ratio while keeping the crystal large enough to easily manipulate for the projects that have been described before. To reach our goal another approach should be taken to utilize the effect of the catalytic potency of the substrate so that the nucleation density and the final crystal shape can be controlled. Wulff-Kaischew theorem states that as the catalytic potency of the substrate increases -which is the adhesive effect of substrate to a particular molecule- the equilibrium shape of the crystal is altered with relation:

$$\frac{\sigma_n}{h_n} = \frac{\sigma_m}{h_m} = \frac{\sigma_n - \beta}{h_m}$$

where σ_n is the surface energy of the surface 'n', h_n is the distance from surface 'n' to the center of the equilibrium shape of the crystal and β is the chemical potency of substrate[59]. If $\beta > 0$, $h_m < h_n$ so that the crystal will be thinner. This effect is visualised in Figure 2.2.

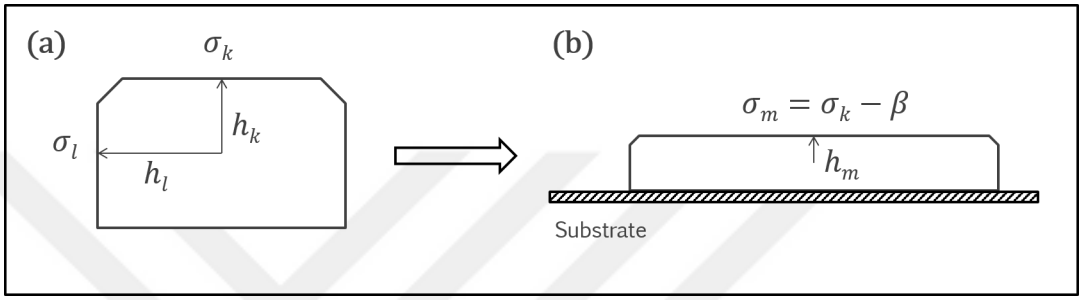

Figure 2.2: (a) shows the crystal equilibrium shape in free space and (b) on a substrate with chemical potency β

As suggested by the Strelcov and colleagues, the surface goes into a reaction with the precursor as:

$$3\ V_2O_5(l) \longrightarrow V_6O_{13}(s) + O_2(g)$$

$$2\ V_6O_{13}(l) \longrightarrow 12\,VO_2(s) + O_2(g)$$

What this means is by controlling the oxygen content of the surface of the substrate, we can control the nucleation rate and catalytic potency of the substrate. This is achieved through sending small amount of oxygen flow before reaching the growth temperature. Another issue to consider is determining the ideal temperature of growth, low temperature would result with lesser nucleation rate and slower crystal growth which would produce small, wire like crystals. Too high temperature on the other hand, would result with thick crystals due to roughening of the crystal surface[60].

2.0.2 Methods

We use a three part furnace made by Protherm that can reach to 1050 °C. V_2O_5 fine powder used as precursor, which is placed in an Alumina boat. The substrate

sits above the Alumina boat with roughly 1 cm apart the precursor, this set up is made to minimize the differences of vapor flux coming from the precursor. For all growths except sapphire, 20($\pm$3) mg precursor is used, for sapphire 10($\pm$1) mg is used; the reason being that 10mg is enough to cover all of the surface of the sapphire surface while for Si, SiO_2 and Quartz substrates 20mg precursor gave better coverage. The growth is divided to two parts, a heat up period and growth period. In the heat up period the furnace is brought to the target temperature in 20$\pm$2 minutes, while giving a predetermined oxygen flow under vacuum.

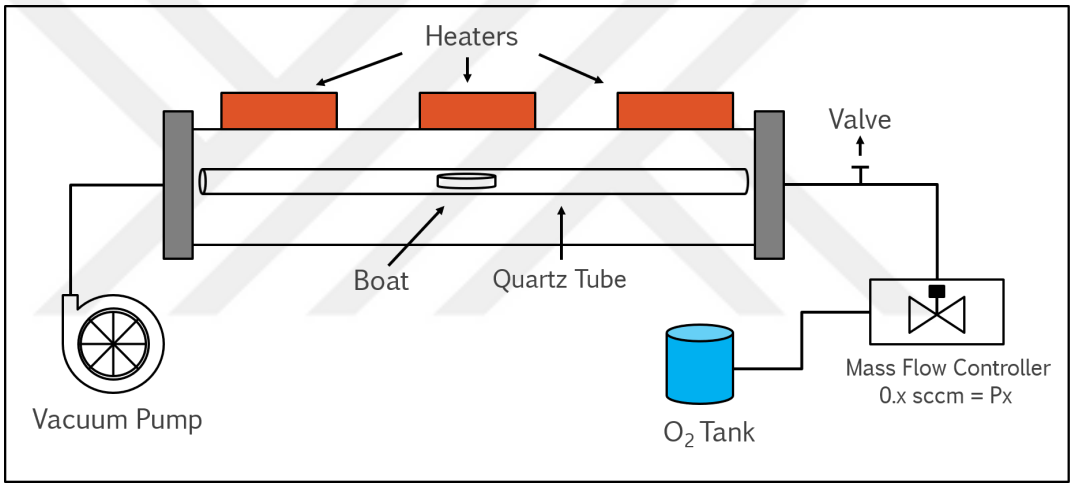

Figure 2.3: Schematics of the growth system

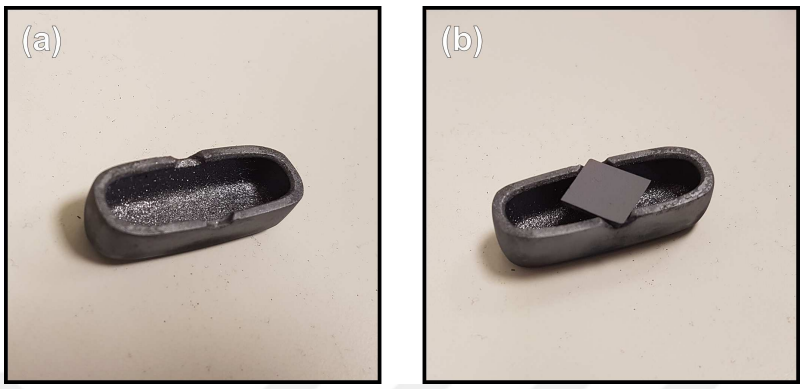

Figure 2.4: Alumina boat used in the growth a) Both sides of the boat is dented to acommodate a 1cm x 1 cm substrate. b) boat-substrate arrangement, substrate stays upside down so that the growth surface directly faces the precursor with roughly 1 cm distance. The alumina boat and the quartz tube acquires a black color after repeated VO_2 growths, but this has no effect on the growth itself and all of our results are repeatable with clean boat and tube.

The amount of oxygen during the heat-up period changes the mode of growth and the Oxygen flow coded as 'Px' which refers to 'x times 0.1 sccm flow rate'. So P5 refers to 0.5 sccm oxygen flow in the heat up period and P3 refers to 0.3sccm and P500 is 50 sccm and so on. The growth types are labeled with centigrades temperature in the front and the flow rate near it. For example in '780-P5' growth, 0.5 sccm Oxygen is given to system in the heat up period and after reaching to growth temperature of 780 °C the flow is ceased. All of the growth is done under vacuum which creates 10^{-2} mbar pressure environment. We use ALICAT SCIENTIFIC brand with MC-100SCCM-D/5M model as our flow controller, and the pressure is measured with Pfeiffer Compact FullRange

Gauge. The pressure values at 750 ^{o}C were,

$$P0 = 1.5x10^{-2}mbar$$
$$P1 = 2.6x10^{-2}mbar$$
$$P2 = 3.1x10^{-2}mbar$$
$$P3 = 3.5x10^{-2}mbar$$
$$P4 = 3.9x10^{-2}mbar$$
$$P5 = 4.3x10^{-2}mbar$$

Another important thing to consider was that the VO_2 growth is very sensitive to oxygen presence in the system so another valve was added at the end of the flow controller in order to seal off the growth chamber after the heat up period. There is a very low amount of leakage that comes from the flow controller which interferes with the VO_2 growth. At the end of the heat up period, the flow is closed and then the valve is closed, then the pressure drops to 10^{-2} mbar in around 30 minutes.

If not specified differently, the growth period time is always chosen as 90 minutes. The substrates are cut with 1 cm x 1 cm dimension then wiped with a tissue wetted with isopropanol and then washed with acetone, isoproponal and D.I. water in that order. Lastly remaining liquids are blown away with N_2 gun.

2.0.3 SiO_2 substrate

For these experiments we have used single crystal (100) Si wafers covered with a $1\mu m$ thick, thermally grown SiO_2 layer. At heat up period, precursor melts and starts to have vapour pressure around 680 °C [2]. The vapour coming from the precursor condense on the surface of the substrate and makes V_2O_5 domes as mentioned before. VO_2 crystals doesn't grow out of these in an instant especially if oxygen is present in the heat up period. To observe the crystal growth stages, four different samples were prepared using 750-P3 route in which the growth stopped and the system was rapidly cooled at different times after the start of

crystal growth period. As it can be seen from the Figure 2.5, the process takes more than 50 minutes. Figure 2.6 shows XPS graphs which support this claim, at 10 minute and 30 minute marks the +4 phase peak which indicates VO_2 presence is not visible.

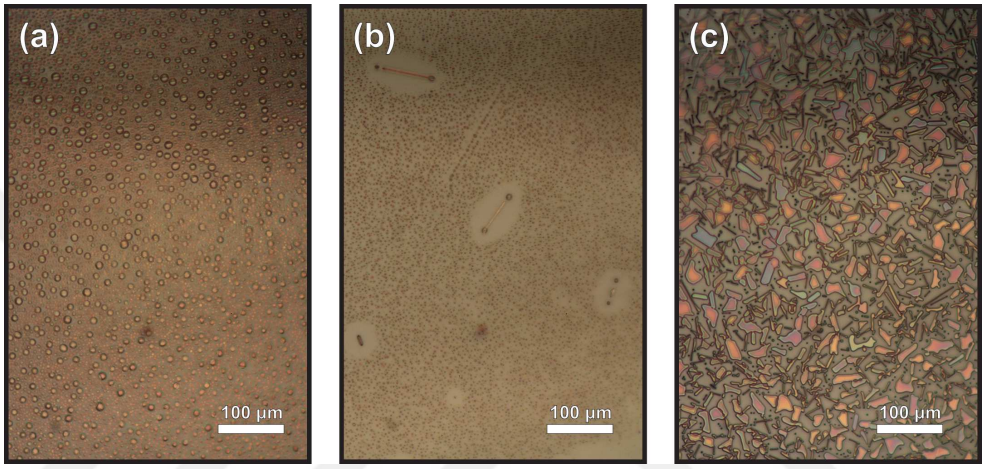

Figure 2.5: Optical microscope images of 750-P3 route stopped at certain times after the start of crystal growth period. Three different samples are prepared which show different moments of growth; a) 10 minutes, b) 30 minutes, c) 50 minutes after the start of crystal growth period.

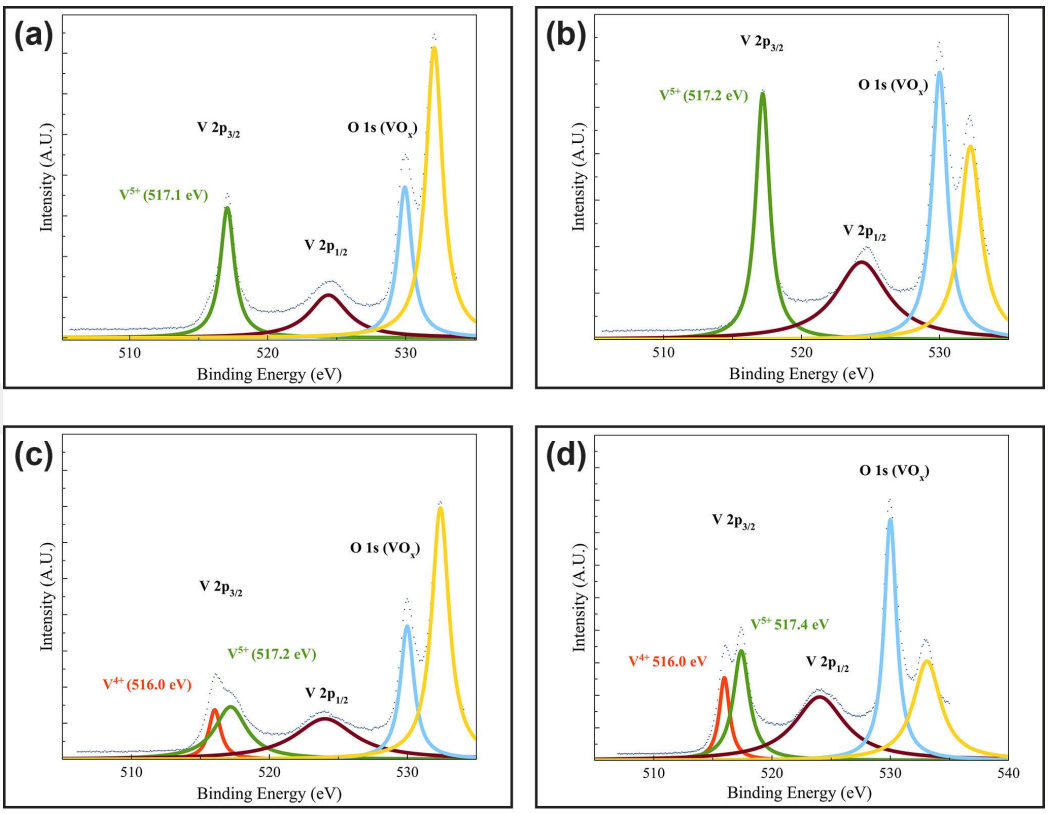

Figure 2.6: XPS analysis of four different samples prepared with 750-P3 route which were stopped at a) 10 minutes, b) 30 minutes, c) 50 minutes d) 90 minutes after the crystal growth period. The O1s peaks are The +4 phase peak from VO_2 doesn't occur after 10 minutes and 30 minutes. Vanadium +5 phase peak coming from The V_2O_5 persist even after 90 minutes due to thin layer of oxidation on the surface of the crystals. The references used for the analysis are: [3][4][5].

Figure 2.7 shows the Scanning Electron Microscope images of the growths that has been stopped after 15 minutes into the ceasation of oxygen flow at 780 °C. When we consider 300nm and above sized dome amounts per area between P2 and P3 routes we see a huge difference. Obviously the critical radius (the radius required for a stable and growing cluster of atoms) required for domes to get larger for P2 is smaller than P3 which helped the domes to get bigger in lesser time compared to P3. We used imageJ software to calculate the diameters of the domes. The silver colored domes in P2 were around 300-446 nm in diameter while P3 silver colored domes were between 400-600nm. The grey domes of P3 were

between 100-200nm. The silver domes connect and start to create line clusters, the lines connecting them are visible under SEM. When we compare P3 and P5, nucleation rate doesn't seem very different but our observation was when we consider connected domes, P3 had larger amount of the low number (2, 3, 4) dome cluster lines compared to P5. In P5 the line clusters mainly had more than 5-6 domes in them. Overall P3 had more line clusters. This may be resulting from line clusters with fewer domes having a harder time to connect and grow at P5. The silver domes of P5 were between 650-790nm in diameter and grey domes were around 160-300nm. Our conclusion is that as more oxygen is in the system during the heat-up period the critical radius of domes also increase.

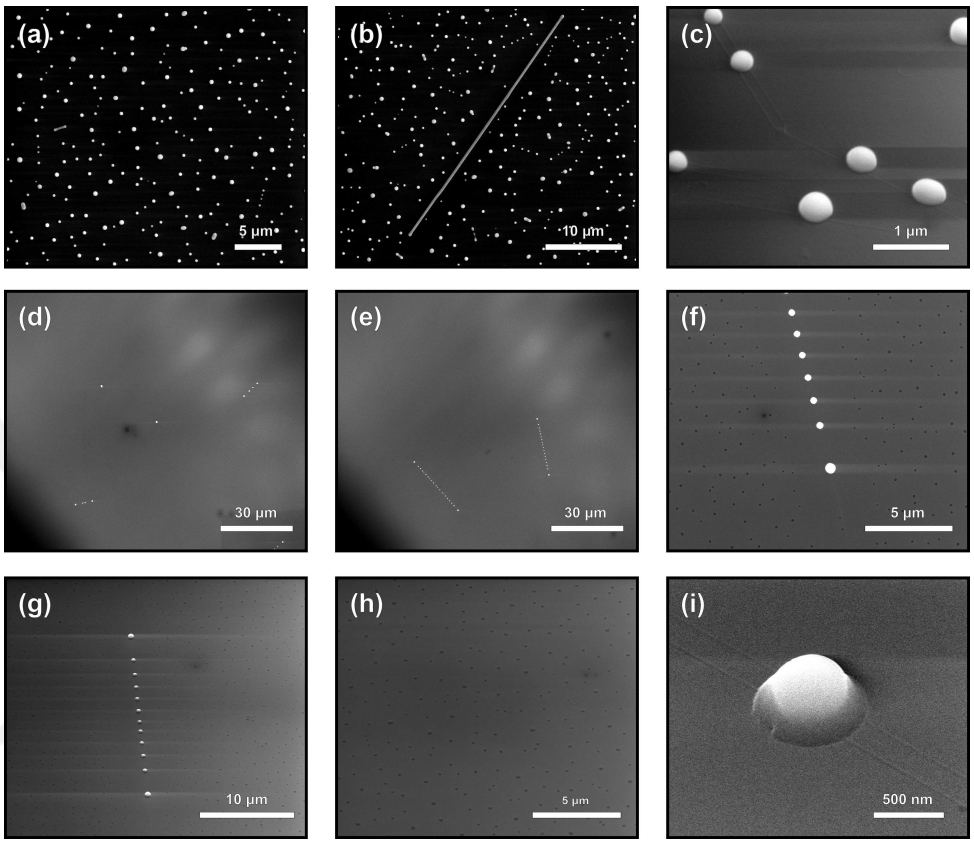

Figure 2.7: Electron microscope pictures of the growths that has been stopped after 15 minutes into the ceasation of oxygen flow at 780 °C. (a), (b), (c) are pictures of P2-780 method. The nucleation rate is pretty high and the domes connect as they come together. The connection lines can be seen at (c). (d), (e), (f) are the images of P3-780 method. The nucleations are much more scarce compared to P2-780. (g), (h), (i) are images of P5-780 method. The nucleation rate is not that much lower than P3-780 but domes that are connected are more scarce.

We have conducted experiments of crystal growth at 720 °C, 750 °C, 780°C and 830 °C with changing oxygen flow values at the heat up period. The Si/SiO_2 substrate surface starts to lose oxygen at temperatures as low as 720 °C under vacuum and without any oxygen flow. However at 720 °C with oxygen flow of P2 at heat up period prevents the loss of oxygen of the SiO_2surface. This makes the surface have higher oxygen concentration which prevents the V_2O_5 domes to

pass its oxygen to the substrate. The result is the suppression of most of the nucleation of VO_2 crystals.

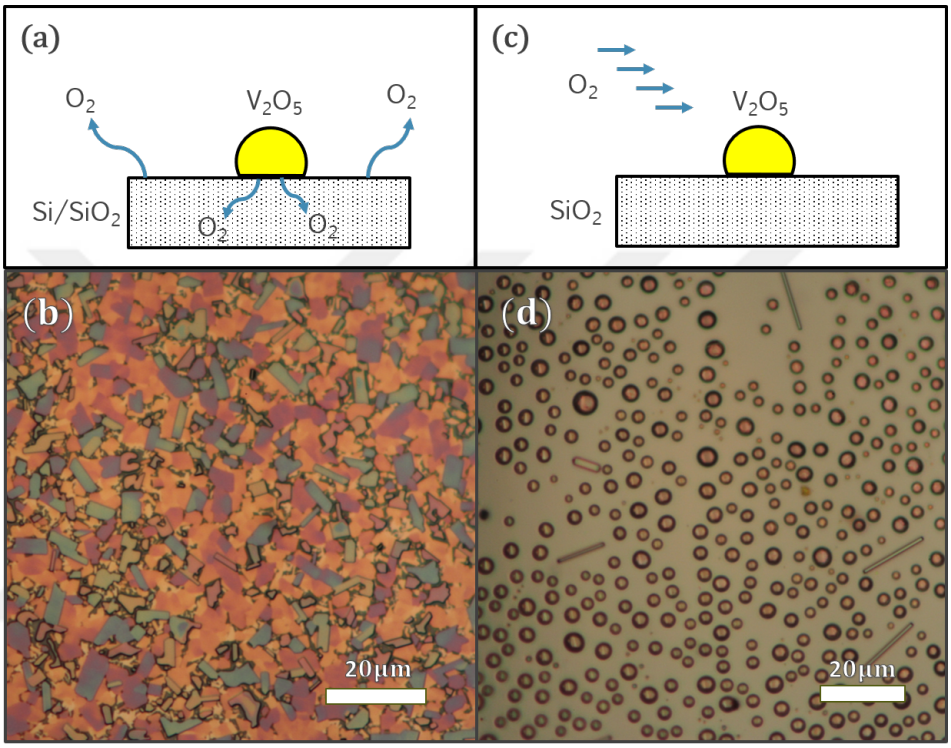

Figure 2.8: With no oxygen flow during the heat up period the SiO_2 surface starts to lose its oxygen and takes oxygen from V_2O_5 domes, starting the nucleation. (a) shows the schematics of this process with (b) showing the optical image of the result, substrate surface fully covered by VO_2. When there is 0.2 sccm O_2 flow during the heat up period, surface of the SiO_2 substrate doesn't lose a lot of oxygen and in turn V_2O_5 domes have much lower nucleation rate. (c) shows the schematics of this process and (d) shows the optical image of the result, the domes mostly stay intact without turning to VO_2. The temperature during the growth period was 720 ^oC for both cases

In all of our experiments from 750 °C to 830 °C, with the increase in oxygen flow at heat up period, a transition from platelet to rod shape happens and nucleation rate drops drastically. For every temperature between 750 °C and 830 °C we get thin platelets at P3 and below oxygen flow values, while it has rod shape at P4 and above. As temperature increases thickness of the platelets also

increase. The white-grey color indicates that the crystal is over 200nm thickness and other colors like red, yellow and blue indicates they are thinner than roughly 170 nm. We also see that compared to P0 or P2, P3 results with larger grain size. The optical images of the mentioned results can be seen below, in figures 2.9, 2.10 and 2.11.

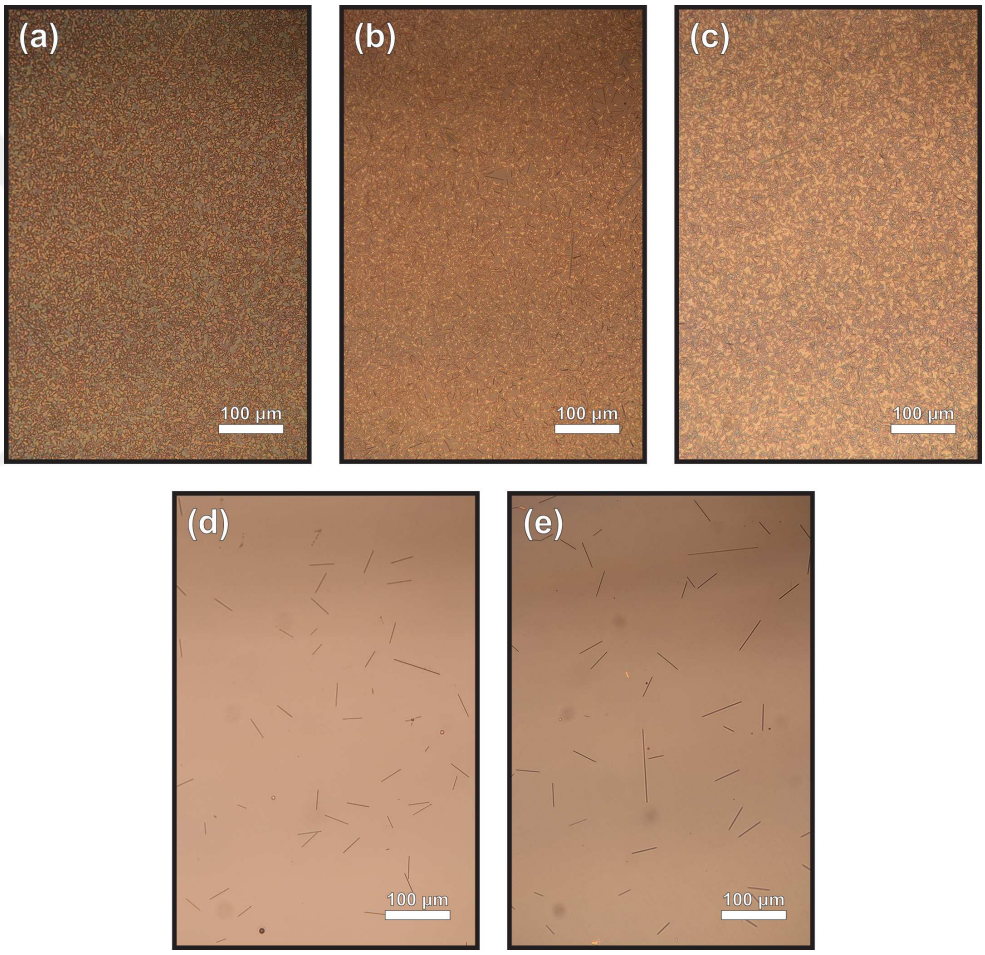

Figure 2.9: Optical images of growth at 750 °C with a) P0, b) P2, c) P3, d) P4 e) P5 routes.

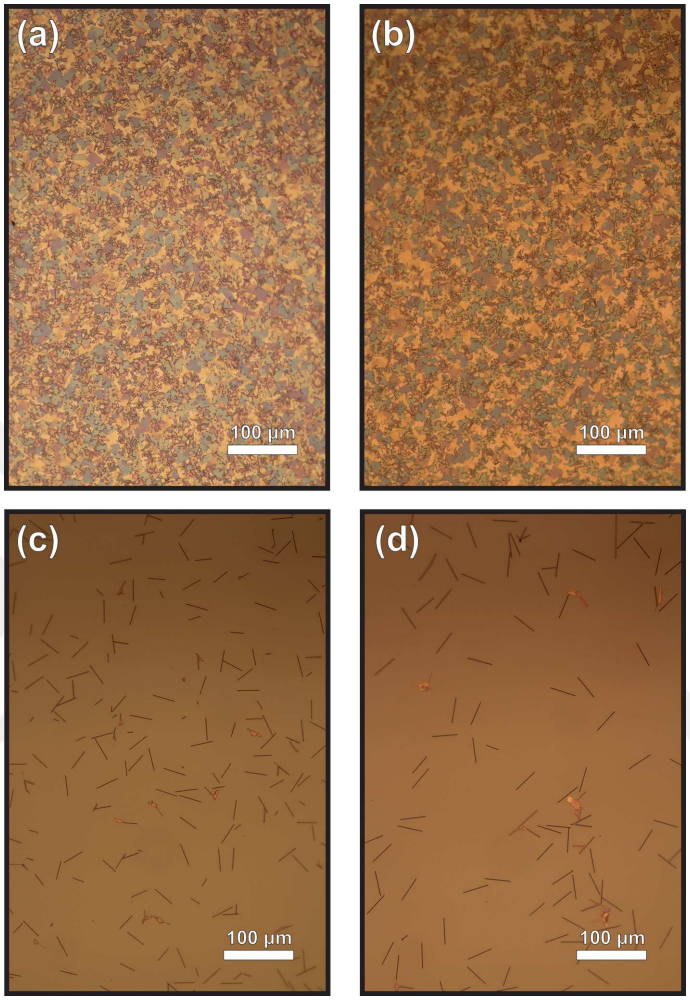

Figure 2.10: Optical images of growth at 780 °C with a) P2, b) P3, c) P4 d) P5 routes.

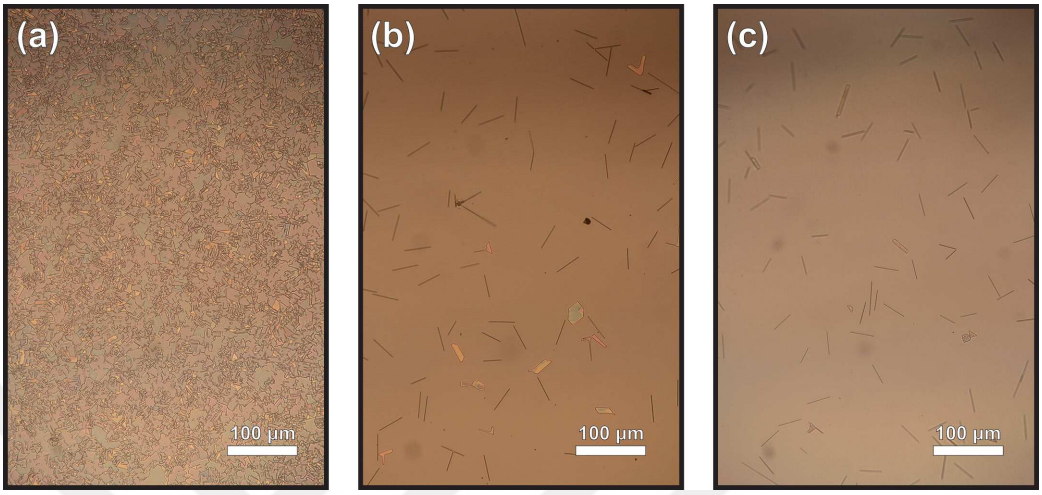

Figure 2.11: Optical images of growth at 830 °C with a) P3, b) P4, c) P5 routes.

The reason of this can't be explained by different deposition rates of the precursor at different oxygen flow values, since the dome density doesn't seem to change with different oxygen flow values. Result of one experiment can be seen in Figure-2.12 where 750-P3 and 750-P5 routes of growth were stopped 10 minutes after the start of the crystal growth period; and the substrates were examined under optical microscope. There seem to be no major difference between dome densities and their radius.

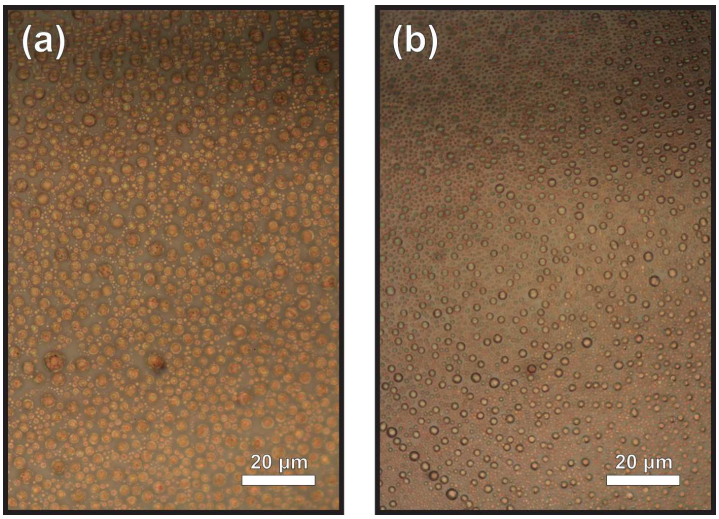

Figure 2.12: Optical images of a) 750-P3 b) 750-P5 routes, the growths were stopped 10 minutes after the start of the crystal growth period.

We argue that the reason of different crystal morphology is due to SiO_2 surface having different oxygen levels at different flow rates which in turn changes the nucleation rate and catalytic potency. If the oxygen level on the substrate surface is low, it is easier for the precursor to lose its oxygen so nucleation rate increases. Due to a mix of the effects of many domes getting connected via growing crystal rods and high chemical potency, we get thin and low aspect ratio crystals and all the surface is covered. When the oxygen level is P4 or high, the surface of the silica substrate is mildly lacking oxygen so it reacts with only a small amount of the V_2O_5 domes thus most of the precursor domes evaporates without forming a crystal. The coverage of the surface is minimal and the preferred growth shape is nanorods. This change is very drastic and the flow change is only 0.1 sccm. At 750 °C, with P3 oxygen flow the oxygen partial pressure is 1.9-2.0x10^{-2} and with P4 it is 2.3-2.4x10^{-2} mbar.

Our hypothetic model is as follows. If the Oxygen value is low enough at heat up period the surface of SiO_2 loses its oxygen and can take the oxygen of the V_2O_5 domes. However at certain oxygen partial pressures for the temperatures between 750-830 °C, the oxygen can't leave SiO_2 surface effectively so that the nucleation rate of domes are very low due to lack of catalytic effect from the substrate. When the nucleation rate is high, almost all of the domes create one and maybe more than one rod nucleations. If one dome has two different rods growing out of it, it may create a suitable bed for two dimensional growth in between the two rods as shown in Figure 2.13(a). This is a result of the precursor wetting the VO_2 surface as mentioned in Figure 2.1. Another possibility is that when almost all of the the domes nucleate, the VO_2 rods can connect with other domes, which creates a growth front in between the rods of these two domes, as shown in Figure 2.13(b). When the nucleation rate is low the domes cannot be connected by rods due to very low possibility of two domes side by side nucleating at the same time. Also the chance of one dome making two rods are almost impossible. This process is shown in Figure 2.13(c).

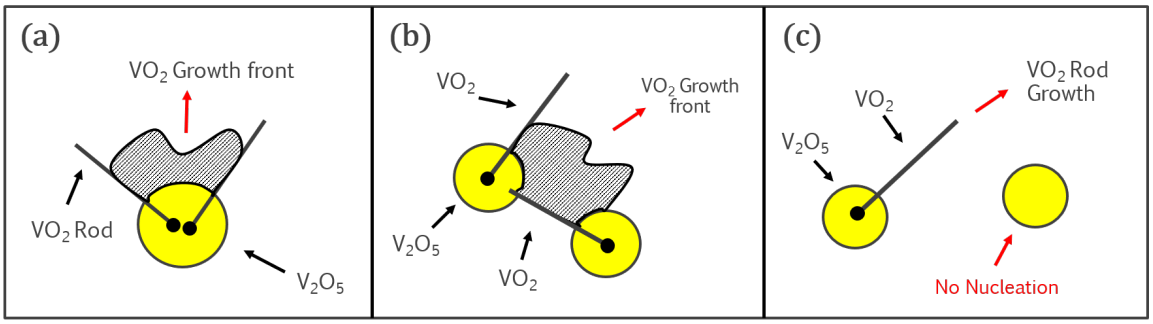

Figure 2.13: Schematics of proposed dynamics of different morphologies seen in VO_2 growth for temperatures between 750-830 °C. (a),(b) shows the x≤3 of Px route where VO_2 platelets cover the surface. (c) shows $x > 3$ where no platelets are seen and the surface is covered with VO_2 rods.

2.0.4 VO_2 growth Methods

As mentioned before for the Hall Effect measurement project, large VO_2 crystals with low aspect ratio was needed. The problem with the growth of P3 and under is that the nucleation rate is so high that the crystals form a continuous layer on the substrate and it is impossible to remove them using a simple needle-manipulator system shown in Figure-2.18. Above P3 however we get one dimensional rods with very high aspect ratio. With the light of the experiments we performed on Si/SiO_2 substrate, we came up with two methods. In Method-1, we tried to increase the nucleation rate using the heating elements of the furnace. where the chamber was heated to 790 °C under vacuum and 0.5 sccm O_2 flow. The pressure stays around $\sim 6x10^{-2}$ mbar during the heat up period. After reaching to 790 °C the flow was ceased so that the pressure is around $\sim 1x10^{-2}$ mbar and then the furnace is heated to 950 °C in 32 mins, in other words 5 °Cmin^{-1} heating rate. The idea is that due to the radiation coming from the furnace, top surface of the precursor droplets would be heated higher than the ambient temperature so that they would nucleate at a higher rate. We had moderate amount of success with creating around 40-60 nm platelet crystals with around 20 μm length but we were unable to remove them physically from the surface of the growth substrate so we didn't investigate more about it. When the crystals are very thin, to remove them

from surface intact other methods like removing with the help of polycarbonate should be used. But the thinness of the crystal might be quite valuable for the TEM studies. Figure-2.14 shows a sample made using Method-1 growth.

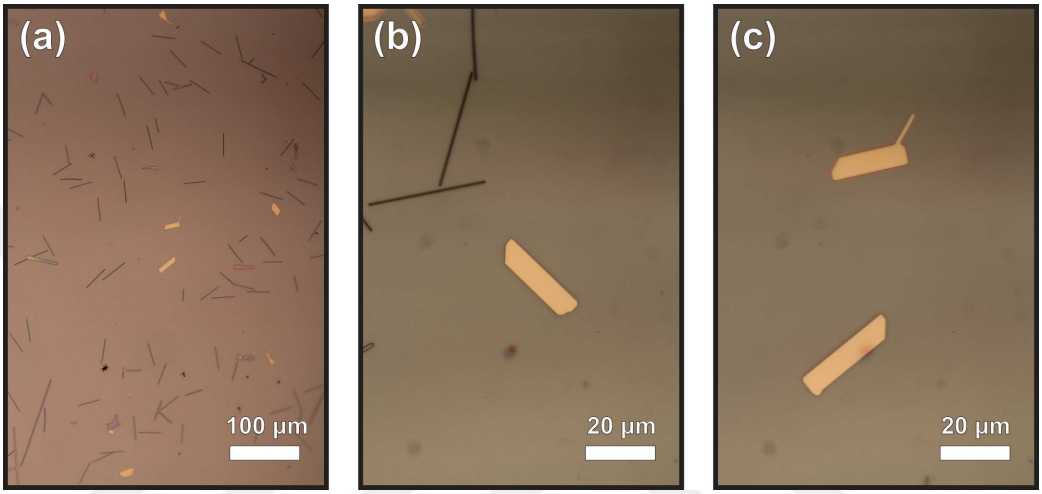

Figure 2.14: Optical image of Method-1 growth on SiO_2 substrate. During the time that the system was reaching to 790 °C, 0.5 sccm O_2 flow given to system. The flow was ceased at 790 °C so while the furnace is heated to 950 °C with a heating rate of 5 °Cmin^{-1}.

In Method-2, We used micro scale particles that would increase the chances of nucleation where they are present, acting as heterogenous nucleation zones. At P5, this results with some precursor domes nucleating very early and connecting other domes before they evaporate, so we get large crystals due to, we believe, the dynamics shown in figure 2.13(b). These crystals are also not connected as in P3 so instead of a polycrystalline film we get large, seperate, single crystal VO_2 beams.

We used a nitrile glove to crete these micro scale particles. After cleaning the SiO_2 substrate, the surface is pressed by the finger of glove which resulted with many particles on the surface. However a certain size and/or number per area is needed to have this effect uniformly so that only one in five-ten growth resulted with high amount of large crystals everywhere on the substrate. On the other hand a good growth can provide around thirty to fifty crystals easily. The foreign

particles don't seem to affect the crystal quality due to VO_2 crystals not showing any difference of MIT temperature and showing very well shaped facets. The TEM results can be seen in the next section where the electron diffraction patterns show single crystal nature of the resulting crystals from this type of growth. And from our experiments, 780-P5 route seem to be the optimum method to grow thin and low-aspect ratio crystals. The crystal thickness was in general between 75nm-170nm. Higher oxygen value during the heat up period or higher temperature at crystal growth period results with thicker crystals. Lower temperature at crystal growth period decreases the amount of platelets and creates higher aspect ratio crystals. This type of Method-2 growth can be seen in figure 2.15.

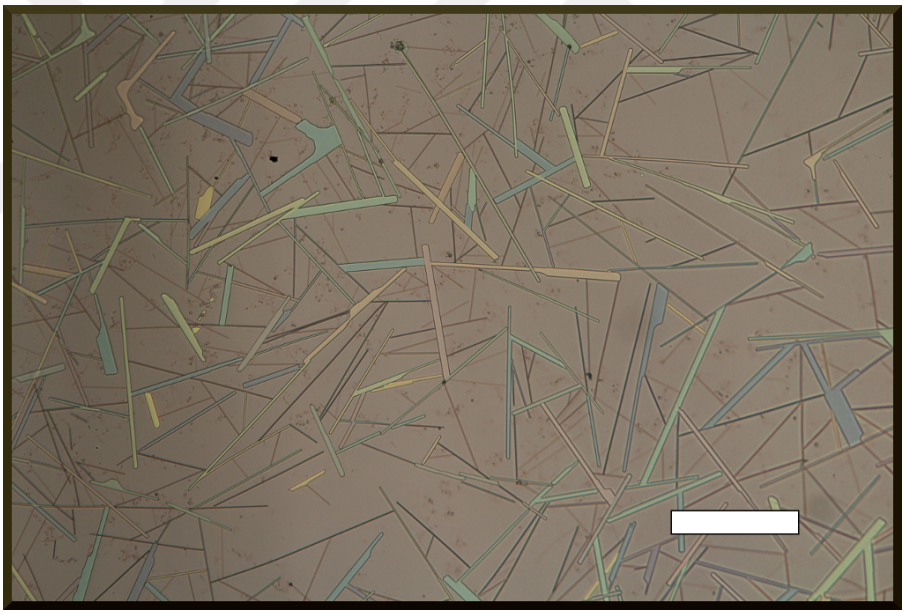

Figure 2.15: Optical microscope image of crystals grown on 1 μm SiO_2 substrate using Method-2 with 780-P5 route. The Scale-Bar is 100 μm.

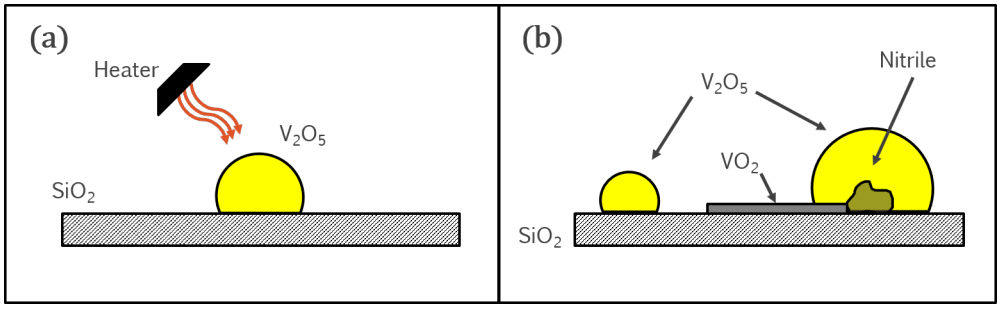

Figure 2.16: Schematics for (a) Method-1 where the radiation coming from the heaters is utilized and (b) Method-2 where particles coming from the nitrile glove are utilized to increase the rate of nucleation and the size of crystals.

All the VO_2 crystals used in the applications mentioned in this thesis are grown on $1\mu m$ SiO_2 substrate using Method-2 with 780-P5 route. These crystals were also routinely utilized for another project in our group where the crystals were transferred on top of exfoliated h-BN flakes. h-BN flakes were exfoliated on $1\mu m$ SiO_2 substrates.

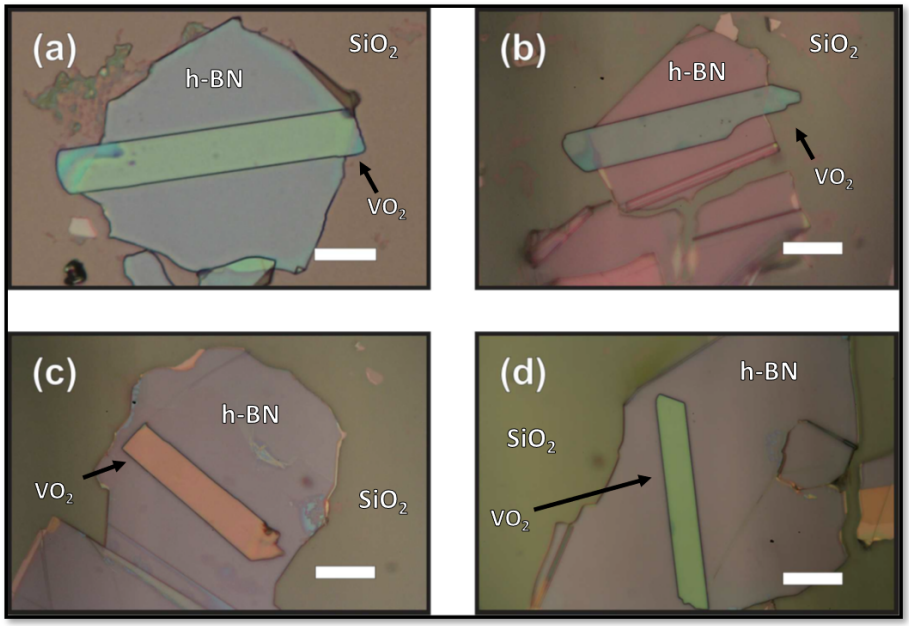

Figure 2.17: Optical microscope images of various crystals grown using Method-2 with 780-P5 route transferred onto hBN flakes for the use in hall-effect measurement devices. Scale bar is 20 μm.

These crystals were transferred using a micro manipulator system. After the growth, the substrates were dipped to buffered hydrofluoric acid (BOE 7:1 (HF : NH4F = 12.5 : 87.5%) for two minutes to ease taking up the crystals using tungsten needle with $1\mu m$ diameter tip attached to micro manipulator. BOE etches the SiO_2 but doesn't etch away VO_2. The micro manipulator system with tungsten needle holder attachment shown in figure 2.18.

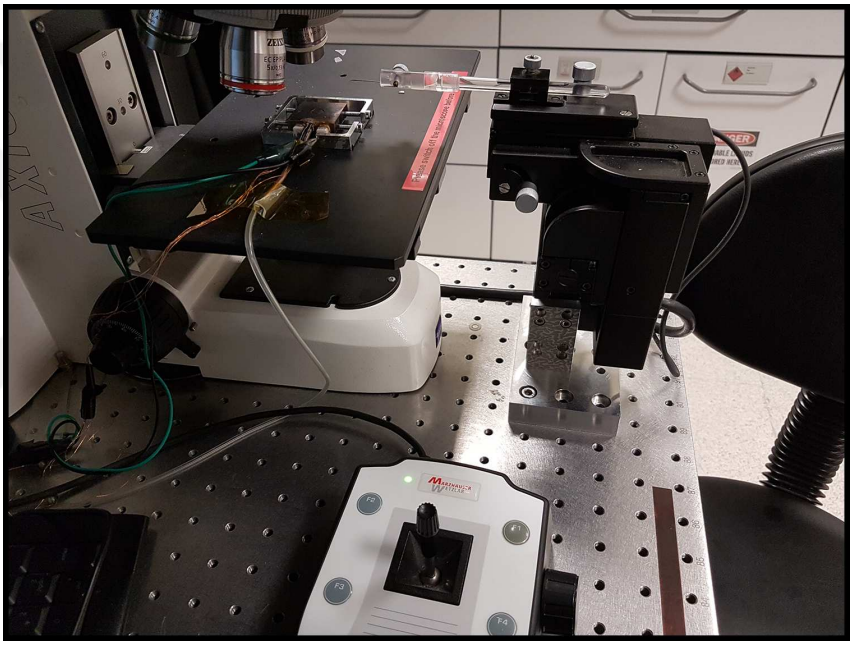

Figure 2.18: Micro manipulator with tungsten needle tip. All of the VO_2 crystals are removed from the surface and transferred using this system. To ease the removing of the crystals from the surface of SiO_2 substrate, the substrates are dipped into 1:7 BOE solution for 2 minutes. If necessary this step is repeated.

2.0.5 Si substrate

We used single crystal <111> oriented p-type(boron as dopant) silicon wafers in these experiments. The catalytic effect of the substrate is much higher in single crystal Si substrates case because of large O_2 affinity of the substrate. With this substrate we observed that the nucleation rate stays high even at P500 growth, but with higher oxygen the thickness of the crystals increase and they become

more three dimensional. We claim that high rates of nucleation at high oxygen levels is due to the diffusion of oxygen from V_2O_5 to the layers under the substrate which means the eutectic layer must be thicker than the oxygenated surface of the Si substrate. But we can effectively nullify the catalytic potency of substrate surface (not the bulk) so that P500 during the heat up period results with the VO_2 crystals not forming platelets but acquiring three dimensional shapes instead, in line with Wulff-Kaischew theorem.

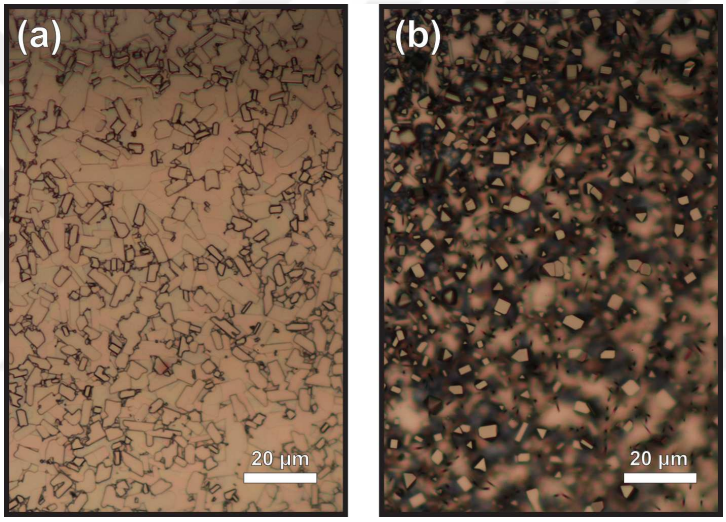

Figure 2.19: Optical microscope image of growth of silicon wafer at 780 °C with a) P5, b) P500 routes.

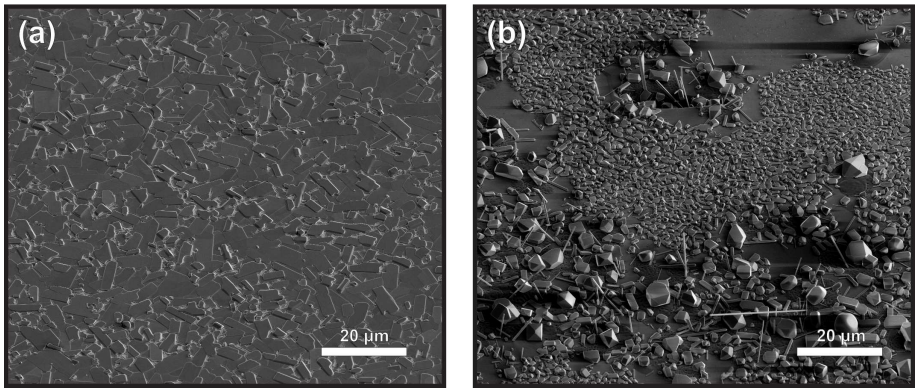

Figure 2.20: Electron Microscope image of growth on silicon wafer at 780 °C with a) P5, b) P500 routes. P5 route shows low aspect ratio thin platelets while P500 shows three dimensional shapes due to low chemical potency of the surface.

2.0.6 Quartz substrate

Opposite of the Si substrate, here the catalytic effect is very low so the nucleation rate is also low. Without oxygen flow the surface is fully covered with VO_2 but P2 route at 780 °C is enough to suppress the nucleation. Given the same temperature and oxygen levels, chemical potency of Si substrate is highest and Quartz lowest with $1\mu m$ SiO_2 substrate in between.

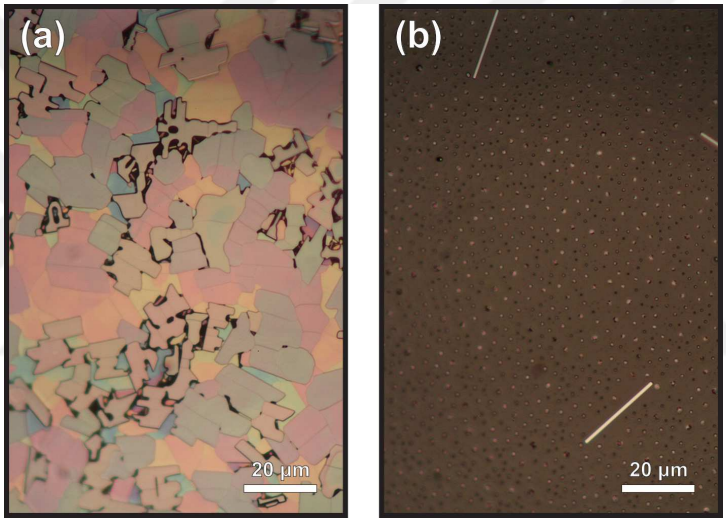

Figure 2.21: Growth on Quartz substrate at 780 °C with a) P0, b) P2 routes.

2.0.7 Sapphire c-plane

Similar to SiO_2 case, supplying oxygen to system at heating period results with lesser nucleation rate. This is probably due to similar mechanisms of growth; in sapphire case there might be a similar reaction that takes place between the surface and the precursor which latter donating its oxygen to the substrate. On the other hand there is an epitaxial relationship between VO_2 and the sapphire surface. V_2O_5 also accumulates on the surface with an ordered structure which might imply another epitaxial relationship. Oxygen provided to system is considerably more than SiO_2 case, mostly between 1-7 mbar partial pressure during the heat up period. When the growth is done under the vacuum

at 750 °C, the surface of the substrate is covered with tiny crystals that are generally not connected to each other. This result is probably the result of two things, slow crystal growth and high nucleation rate. We would expect the same morphology at temperatures between 750-850 °C but we don't have records for other temperatures. When oxygen is supplied during heat up period, the density of nucleation sites decrease but the length of the crystals grow considerably, which can be seen in figure 2.22 (b).

Interestingly, if the temperature is raised during the growth period(Method-1), we get the best results. Increasing temperature during the growth most likely raises the supersaturation of the V_2O_5 domes on the substrate by heating them to a higher temperature compared to the growth period temperature. So the V_2O_5 domes nucleate faster but the temperature most likely becomes same with the system at the time of crystal growth. The result is that the nucleation rate is enhanced and nucleation occurs earlier compared to the 850-P5 route. This results with crystallization also beginning earlier so that a larger amount of precursor turns to VO_2 instead of evaporating as in 850-P5 route.

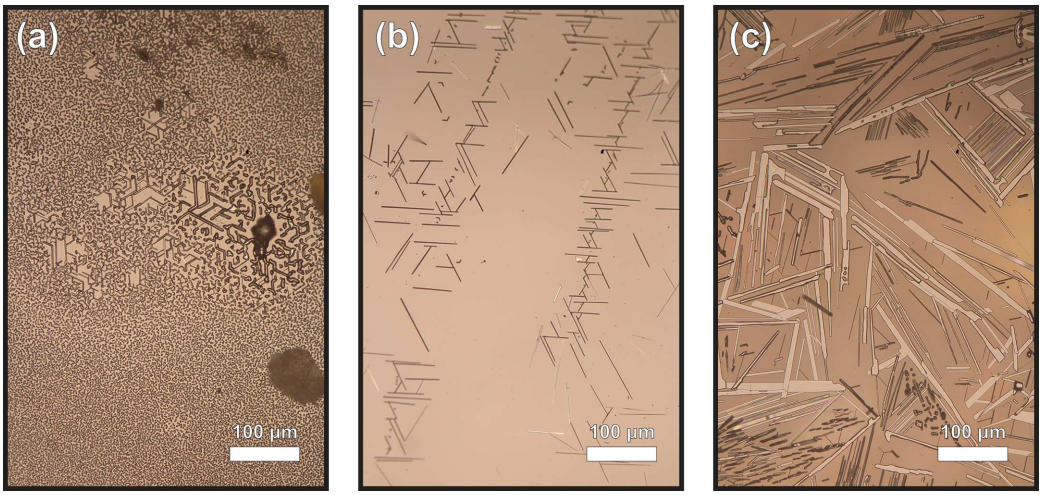

Figure 2.22: Optical microscope image of VO_2 on c-cut sapphire. (a) No oxygen flow given to system at heat up period and the temperature was 750 °C at growth period, (b) 1:3 O_2:Ar flow provided to the chamber during the heat up period and c) 1:3 O_2:Ar flow provided to the chamber during the heat up period till 750 °C then temperature is raised to 850 °C with rate of 10 °C/min.

We also observed Vertical growth of VO_2 with many different morphologies using Method-1 with Sapphire c-plane substrates. Sohn and colleauges showed in their work that the vertical growth of VO_2 is seen on a-cut and r-cut sapphire but not on c-plane [46]. Because they grow in certain places and considering the results of a-plane and r-plane we came to conclusion that they occur because of existing steps on the substrate. This suggests that with different miscuts on c-plane we can get different morphologies of vertical VO_2 crystals. These growths can be seen in figures 2.23 and 2.24.

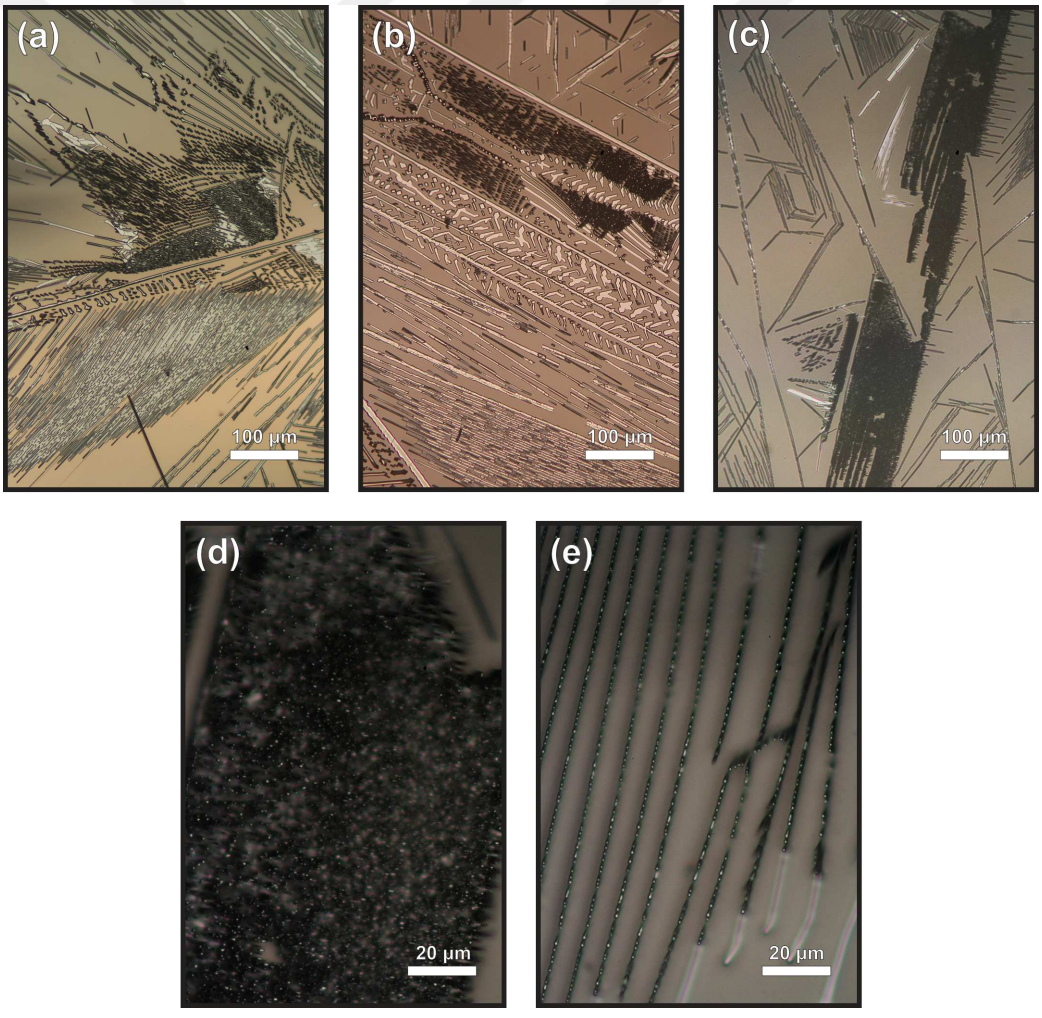

Figure 2.23: Different modes of growth under optical microscope, with VO_2 beams and vertical rods. Vertical rods cast shadows on the substrate.

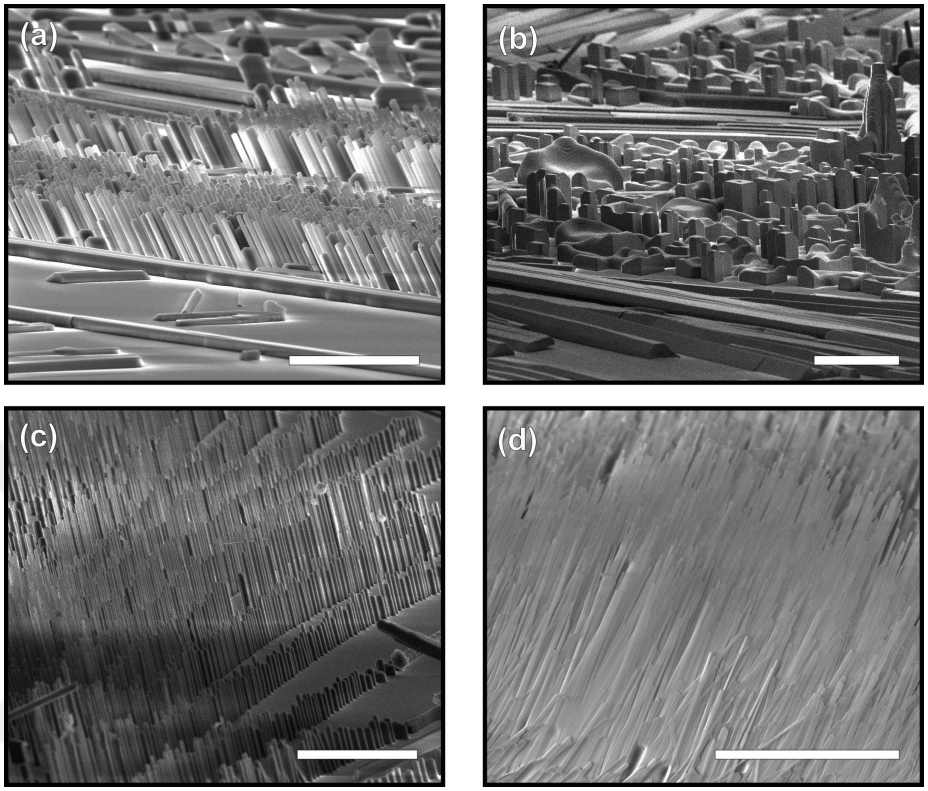

Figure 2.24: Different morphologies of VO_2 under electron microscope that were grown on sapphire c-plane substrate. All the scalebars are $20\mu m$.

Both are seem to be epitaxial growth of VO_2, similar to the growths reported by Sohn and colleagues [46]. As layed out in Sohn et al's work the epitaxial relation between VO_2 and c-cut sapphire is (010) VO_2//(0001) sapphire and our XRD measurement shows that our growth has 39.9° (020) and 85.9°(040) signals of VO_2. The indexing is done using Pearson's Crystal Data.

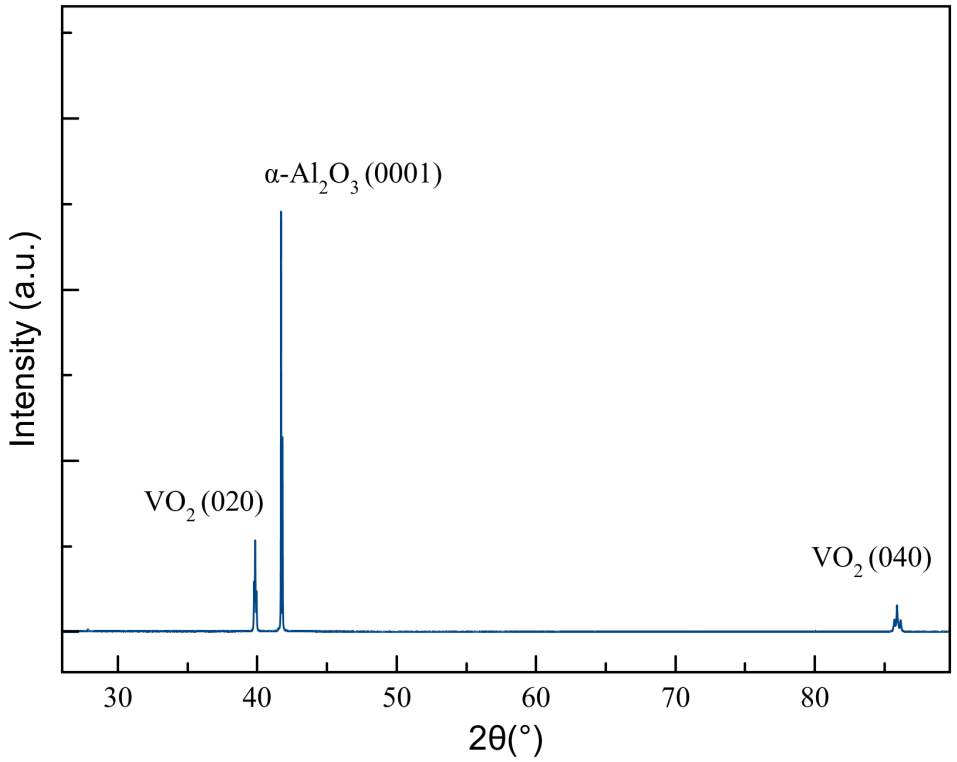

Figure 2.25: XRD results for VO_2 growth on c-cut sapphire. During the heat up period a growth 1:3 O_2:Ar flow provided to the chamber till 750 °C then temperature is raised to 850 °C with 10 °C /min. a.u.: arbitrary units.

Chapter 3

TEM Studies of Hydrogen Doped Crystals

The metal-insulator transition of VO_2 crystals can be modified by atomic hydrogen Doping using catalytic spillover method. At temperatures above 65 °C, atomic hydrogen enters from the tip of the crystal which is [001] direction of the rutile phase [37]. The hydrogen atom can only enter through the lattice openings that exist only in the (001) plane of the rutile phase of the crystal.

As Chippindale and his colleagues demonstrated in a 1991 study, this results with MIT disappearing from the system with another metallic system staying thermodinamically stable at room temperatures. They mention doping is quite slow under 90 °C and improves significantly after that value which we also observed. These doped compounds which referred as H_xVO_2, changes its crystal structure with changing x values. Between $0 \leq x \leq 0.08$ it stays at monoclinic phase but for values $x>0.08$ the crystal structure becomes orthorombic and lattice parameters change with differing x values[40]. Filinchuk et al. further improves this with dividing the orthorombic structures to two phases, O1 and O2, O1 being the phase not having ordered hydrogen positions and O2 being the one with ordered hydrogen positions[39].

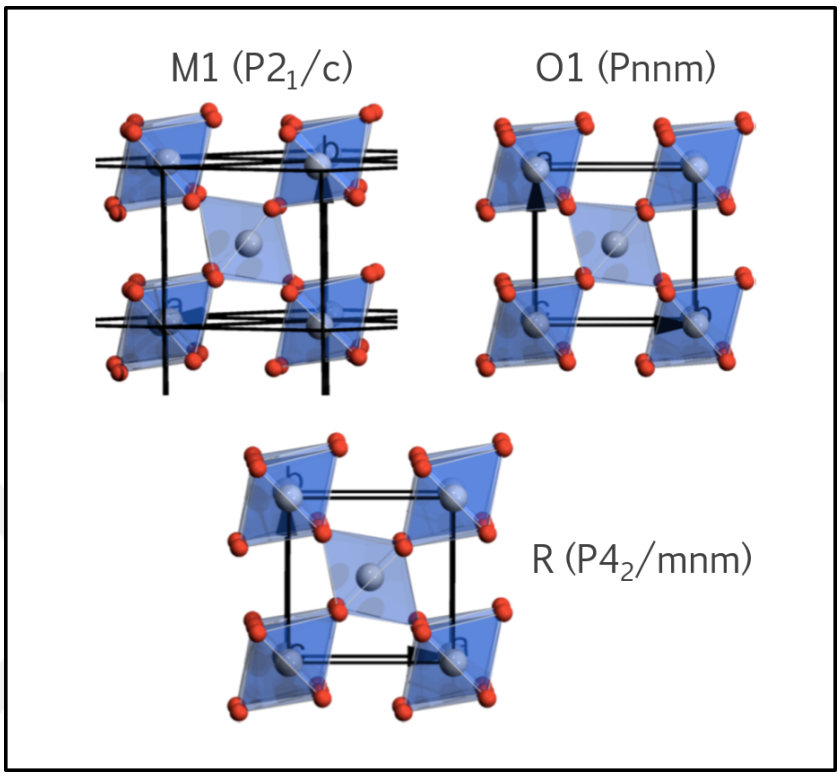

Figure 3.1: The monoclinic (M1), tetragonal-rutile (R) and orthorhombic (O1) structures of VO_2 are shown, looking from the c-axis for R, O1 structures and slightly misaligned a+c direction for M1. Oxygen atoms are colored red and Vanadium atoms are colored grey. Below the transition temperature, VO_2 crystal has monoclinic(M1) structure and above it has rutile(R) structure. With hydrogen doping the lattice structure turns into orthorombic structure with 'b' lattice constant of rutile structure getting larger. Reprinted (adapted) with permission from (Filinchuk, Yaroslav, et al. "In situ diffraction study of catalytic hydrogenation of VO2: Stable phases and origins of metallicity." Journal of the American Chemical Society 136.22 (2014): 8100-8109). Copyright (2014) American Chemical Society.

As the H_xVO_2 crystal receives more hydrogen, the O1 phase turns into O2. O1 phase has Pnnm space group with lattice constants a = 4.4795(12), b = 4.7372(11), and c = 2.8944(5) Å, compared to VO_2(R), the b lattice constant is larger(b=4.554Å for the rutile phase). O2 phase has Fdd2 space group with

lattice constants a = 8.9309(13), b = 9.4285(19), c = 5.7652(6) Å.

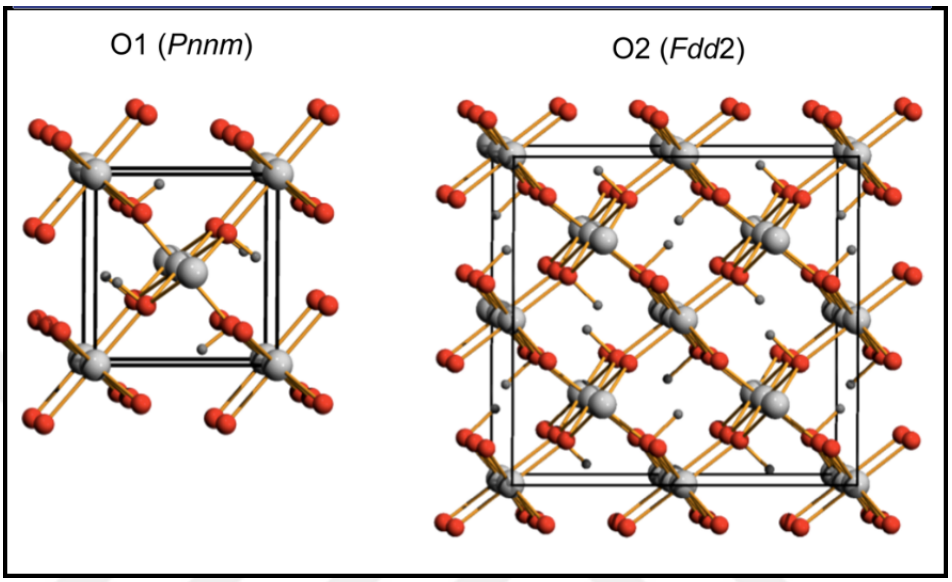

Figure 3.2: Orthorhombic (O1) and (O2) structures of VO_2 are shown, looking almost down from the c-axis. Oxygen atoms are red spheres, vanadium atoms are the large gray spheres and hydrogen atoms are the small gray spheres. In the O2 phase the hydrogen positions are ordered which is not the case for the O1 phase, but here they are shown ordered for illustrative purposes. Reprinted (adapted) with permission from (Filinchuk, Yaroslav, et al. "In situ diffraction study of catalytic hydrogenation of VO2: Stable phases and origins of metallicity." Journal of the American Chemical Society 136.22 (2014): 8100-8109). Copyright (2014) American Chemical Society.

Since the hydrogen enters from the tip and diffuses through the direction of c-axis, these crystals can have both orthorombic and monoclinic structure stable on the same single crystal at room temperature after doping. These different crystal structures have different colors divided with a distinct boundary that can be seen under the optical microscope. We could produce crystals that are generally between 75nm-170nm and they have different colors with changing thicknesses. The doped parts also have distinct colors with changing thickness.

Our aim in this study was to investigate how the crystal structure changes at

the boundaries. We wanted to see if the hydrogen saturation in the crystal was same all around at the doped parts, that is to say if the hydrogen diffusion speed variation was negligible. Also we wanted to see the difference of diffusion speed along the c-axis compared to across of it. In order to realize these we blocked half of the tip of the crystals. So this would mean there would be a boundary layer both parallel and perpendicular to (001) direction of the rutile phase. This is done by covering half of the crystal with 20nm-40nm Platinum. To remove the oxidated layer in front of the tip, the crystal is dipped into buffered oxide etch(BOE) and then to protect from further oxidation the tip is coated with 4nm Palladium at thermal evaporator. Both palladium, and platinum membranes can dissociate and dissolve hydrogen, but because of its high hydrogen solubility only palladium membranes show an outstanding ability to transport hydrogen at a wide range of temperatures [61]. Platinum on the other hand, even at 500 °C, for every 10^5 atoms of platinum 1 atom of hydrogen is present [62]. This means at low temperatures we use, Pt coating acts as a barrier for hydrogen.

3.0.1 Methods

The crystals are grown on the 1 μm SiO_2 with 708-P5 fingerprint method. Crystals are transferred to a TEM grid, a commercial copper one or a gold one we have designed. The crystals are attached to the grid using 100-150 nm thick Pt using Focused Ion Beam. Covering the half of the tip with 20 nm Pt is also done at this stage. The samples are then dipped to 1:7 BOE solution for 30 seconds to remove the oxide layer that develops in air environment. After the treatment samples are directly taken to thermal evaporater for the Pd coating. If the crystals wait too long without Pd coating the oxide layer redevelops. The TEM samples are placed in the thermal evaporater in a way that the tip faces the coming flux of Pd atoms. The schematics of the processes are shown in figure 3.1.

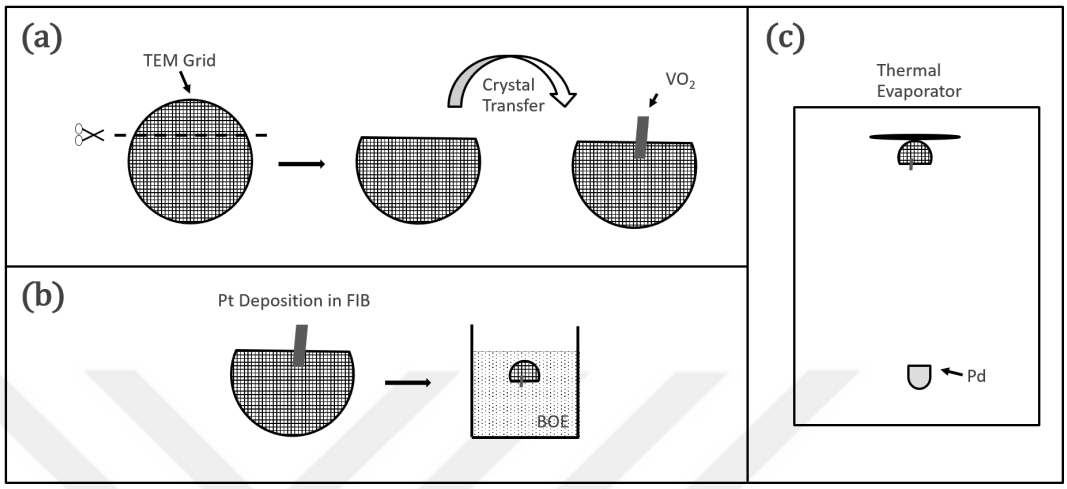

Figure 3.3: The processes for making of the TEM samples is as follows: (a) First TEM grid(copper or gold), is sliced to two parts using scalpel which makes it easier to transfer VO_2 crystals and knowing the orientation of the crystal for Pd deposition. The VO_2 crystal is then transferred onto the TEM grid. (b) After the transfer is done, the TEM sample is taken to FIB where the sample is attached to the grid from its tail, sitting on the grid, using 100-150nm Pt deposition. Half of the tip is also covered with 20nm-40nm Pt. After this step the sample is dipped to 1:7 buffered oxide etch(BOE) solution to get rid of the oxidation on the surface of the crystal. (c) Immediately after the treatment of BOE, the sample is taken to thermal evaporator to cover the tip with 2-4nm of Pd. Because the flat of the grid and the flat part of the crystal tip are made to be parallel, we can adjust the placing of the sample in a way that the tip faces the coming Pd flux.

The attachment of the crystal to grid using Pt deposition via FIB may create some bending of the crystal. So the crystal should be in full contact at the point of attachment.

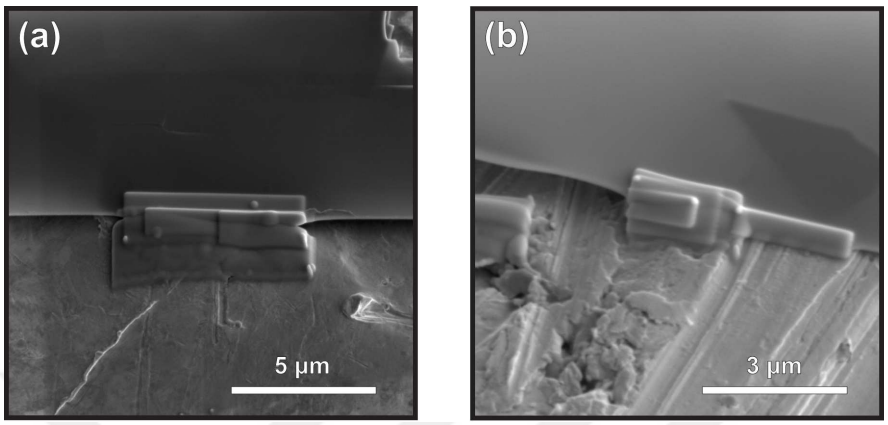

Figure 3.4: Bending caused by Pt deposition. This bending can be minimized by depositing Pt from the sides that have full contact to the TEM grid. It is also important to attach them from only one point.

After these treatments, we dope the crystals with hydrogen at ambient pressure in a chamber where we heat the sample to 100-120 °C. During the heat up period constant argon flow is kept to flush the system from air. During the doping, a constant ratio of argon and hydrogen flow is given to system which we will discuss in the results section. The schematics of this process is shown in figure 3.4.

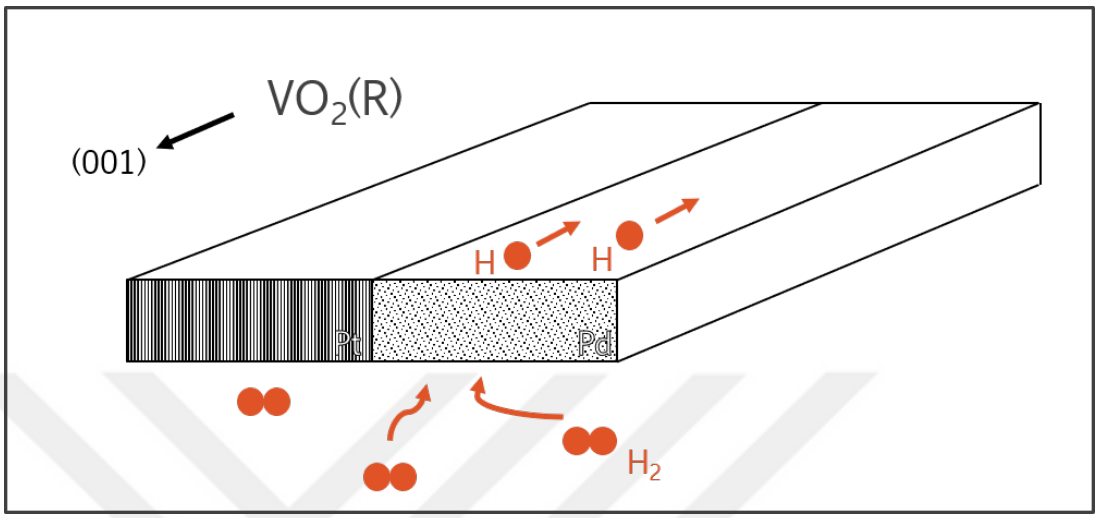

Figure 3.5: Schematics of the doping and the functionalized VO_2 crystal that allows for the doping of only one half of it. The 20-40nm of Pt covered half of the tip doesn't allow the passage of hydrogen atoms while Pd coated half acts as dissociative hydrogen membrane which dissociates the hydrogen molecules and diffuses resulting hydrogen atoms which goes inside along the Rutile(001) direction of VO_2 crystal.

Since there are a lot of operations involved to prepare a crystal for TEM, thin and fragile copper grids are not very suitable for this application. However we have created many samples with thin copper grids resulting with loss of a part of my sanity. Later into our studies, we started to use a custom made gold TEM grid made from 0.3 mm thick gold plate and with dents created by a razor blade.

The bending problem caused by attachment of the crystal to the grid using Pt deposition cannot be removed completely. The hydrogen doping is also problematic since the doping causes a lot of stress in the crystal which in turn bends the crystal. This was the main problem we have dealt with. As it can be seen from figure-3.5 the line between the doped and the undoped part is under huge stress and taking Selected Area Electron Diffraction (SAED) or High Resolution TEM data are impossible due to bending.

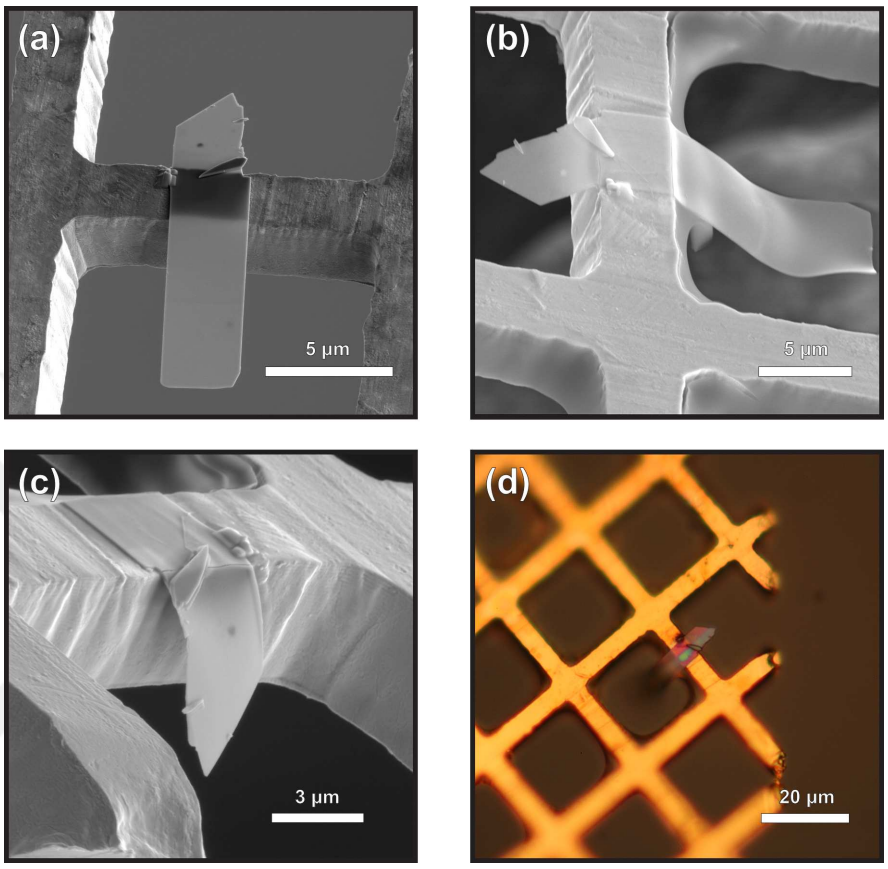

Figure 3.6: (a) SEM image of VO_2 single crystal before doping. b,c) same crystal after doping at 150 $^{\circ}C$ with 30 sccm H_2 and 60 sccm Ar flow for one hour. d) Optical microscope image of the same crystal after doping, the blue part is undoped VO_2 and the magenta part is hydrogen doped H_xVO_2.

To minimize the bending, we have lowered the temperature and the hydrogen amount during the doping. Also we transferred the crystals with most of the crystal body siting on the grid so that some of the bending is neutralized by the grid. This worked well enough that we could get TEM Selected Area Electron Diffraction (SAED) pattern images and HRTEM images.

3.0.2 Results

Most of our transfers were around 100-120 nm so these crystals were not suitable to analyze in TEM though some charecteristics of half doping can still be realized from them. Figure-3.6 shows a crystal that is around 140nm transferred onto a copper grid, to the resulting assembly we call the 'Copper TEM Sample'. Our preperation method is different for this and only this crystal, and it is as follows: First a $1\mu m$ SiO_2 substrate is used for a growth of Method-2 780-P5 route. After the growth the substrate is dipped to 1:7 BOE solution later it was put into thermal evaporator. The substrate was placed with an angle so that tips of some of the crystals on the substrate would face the incoming Pd flux. After the coating the substrate was doped for 2 hours and 40 minutes with 30 sccm H_2 and 90 sccm Ar flow at 113-116 $°C$. Then a half doped crystal was chosen from the substrate and transferred onto a copper grid. This amount of doping is normally too much comparing to our samples which were first transferred then coated with Pd with the crystal tip is facing the Pd flux.

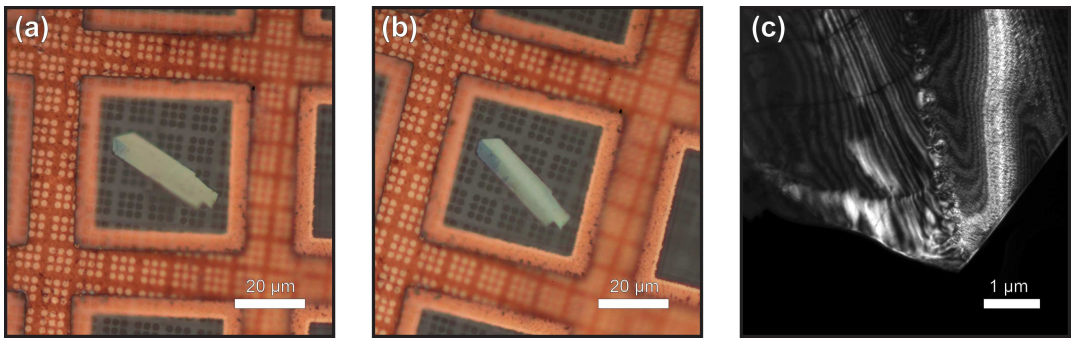

Figure 3.7: Optical image of VO_2 crystal sitting on Copper TEM Sample after doping for (a) 40 mins, (b) after 2 hours(+40 minutes). The darker colored area shows the doped part. (c) SEM image of the same crystal with the stress line in the middle.

For TEM, in general samples should be under 80 nm for the electrons to penetrate. One of our transfers coming from a 780-P5 fingerprint growth was a 75 nm crystal. The crystal is transferred to the custom made Gold grid. After coating with 20nm Pt from half of the tip and then coating the other half with

4nm Pd from the tips, it is doped with 10 sccm H_2 and 50 sccm Ar for 30 minutes at 120 $°C$. They got bent, but it was still possible to take some TEM data. This was because only a small part of the crystal body was sticking out of the gold grid so the rigid body was preventing the crystal from crumbling.

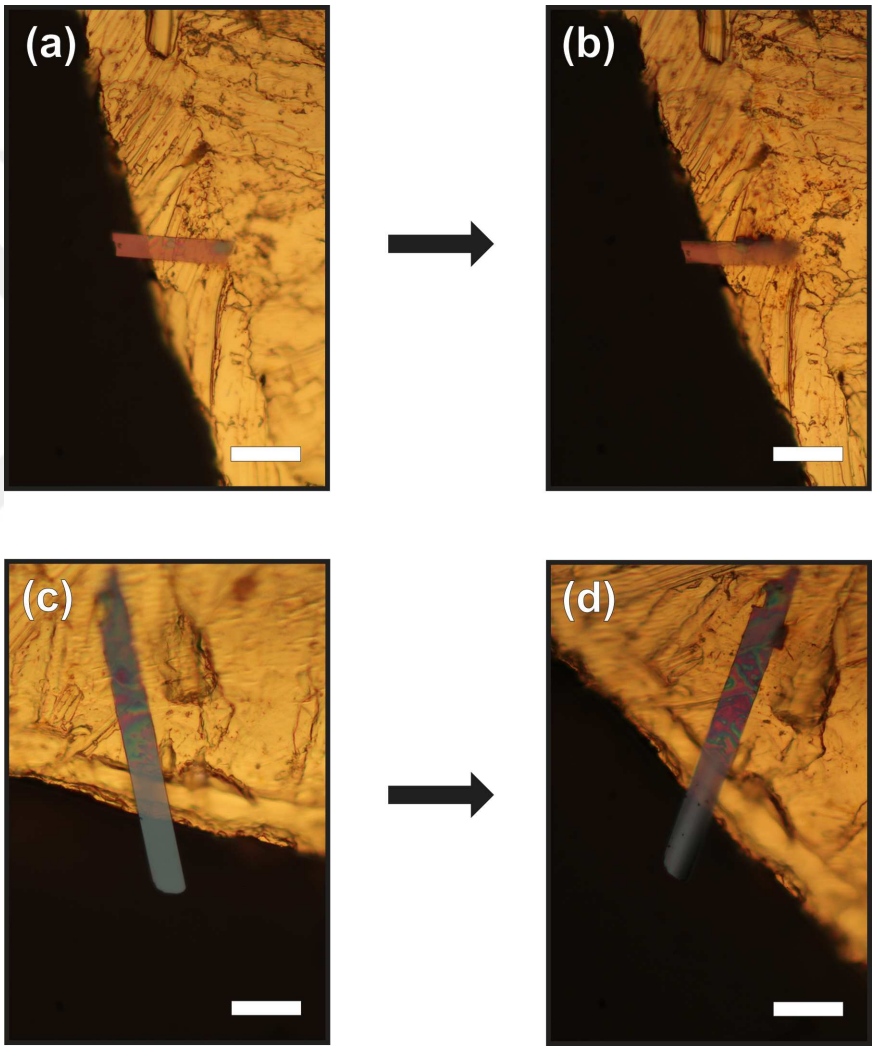

Figure 3.8: Optical images of TEM assembly called the Gold Sample. (a), (c) are crystals transferred onto the same custom made gold grid. Crystal in (a) is 75 nm and (c) is around 110-120nm. (b), (d) are taken after the hydrogen doping at 120 $°C$ with 10 sccm H_2 and 50 sccm Ar. Scale bar is 20 μm.

As it can be seen from our diffraction data the crystal is single crystal and the undoped part seems to exhibit monoclinic phase $P2_1/c$[21]. This result should be

taken with a caution because the indexing was done by hand and we couldn't take more data due to bending of the crystal. We've used the stereographic projections created by WinWULFF software of JCrystalSoft and the d-spacings that were calculated by using the basic d-spacing formulas for monoclinic and orthorombic structures using paper of Filinchuk et al. for O1-O2 phases[39] and demo version of Pearson Crystal Database.

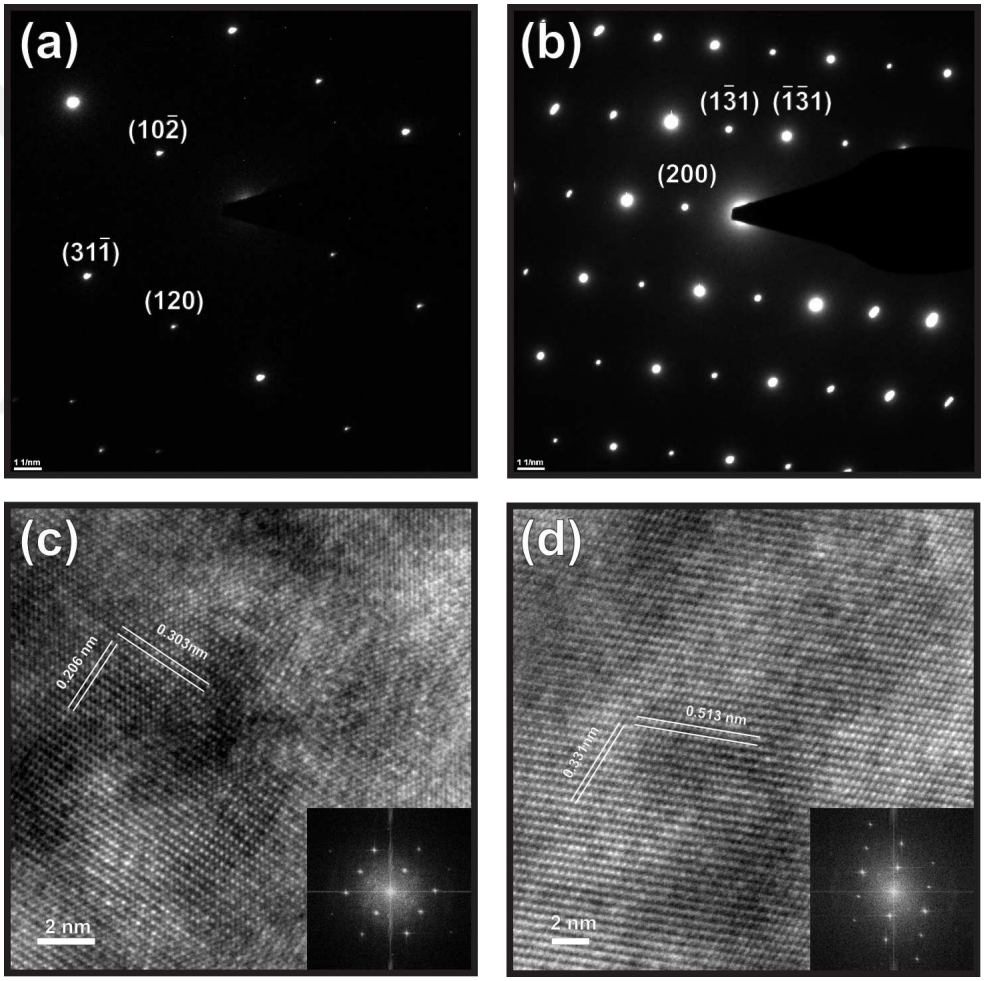

Figure 3.9: SAED patterns and HRTEM images of 75 nm crystal on the Gold Sample. (a) is the undoped part with monoclinic $P2_1/c$ phase and (b) is the doped part with O2 orthorombic phase with Fdd2 space group.

The doped part seems to show a face centered structure which fits to orthorombic O2 phase with Fdd2 space group mentioned in Filinchuk et. al.

paper however with some differences[39]. If our indexing is correct, the $1\bar{3}1$ layer distance is too low and the angle between $\overline{1}\overline{3}1$ and $1\bar{3}1$ is slightly smaller which indicates that their lattice constant 'b' is too low. In their paper they use powder form of VO_2 coated with Pd nanoparticles for the molecular dissociation and catalytic spill over of hydrogen and they reach to O2 phase with 15 bar of hydrogen pressure at temperatures 195 $°C$ for 2 days. It seems like directly coating the tips with 4 nm Pd is a lot more efficient so that we could reach this phase in just 30 minutes at 120 $°C$ while having more hydrogen atoms inside so the 'b' lattice constant grew larger.

Chapter 4

Electronic structure changes in VO_2 crystal with hydrogen doping

To study the change in electronic properties of VO_2 crystals as it is doped with hydrogen, we have developed an experiment in which we can observe both the resistivity and the different phases of VO_2. As it is described in the previous chapter, by coating the tip with 4 nm Pd we can effectively dope the crystal with hydrogen only from one side so while having a very efficent hydrogen doping we could also see the line that seperates the orthorombic state and monoclinic state which would be visible under the MIT temperature. A similar device can be found in the work of Baik et al., where they have successfully demonstrated a highly responsive hydrogen sensor using a VO_2 nanowire. However in their device Pd is not coated on the tips but randomly dispersed which might make the hydrogen spill-over to crystal less effective. Another difference in our aim was observing the interplay between the orthorombic phase and the monoclinic phase, If the resistivity drops only after some time and raises to a limit linearly it means that all the hydrogen atoms move as an entity so a diffusion time can be defined. But if the resistivity were to start to drop immediately and then reach a saturation that would mean that hydrogen diffusion rate is non-linear may depend on many

factors.

4.0.1 Methods

The crystals that were used in this project was remaining attached to the surface of growth substrate. First the crystals were patterned as a 2-terminal device with Electron-Beam Lithography (EBL). After patterning with 5 nm Chromium and then 100 nm gold in E-Beam Evaporator, the crystal was dipped to BOE to free them from the surface so no unnecessary stress would be present to alter its electronic characteristics. The crystal stayed in BOE for 8 minutes to free it from the silica substrate then 4 nm Pd is evaporated to the tip of the crystal using thermal evaporator using techniques mentioned before. After wire bonding the sample was placed in a home-made chamber in which we can heat the sample and observe the process of doping optically and keep a constant gas flow. Some of the prepared devices can be seen below.

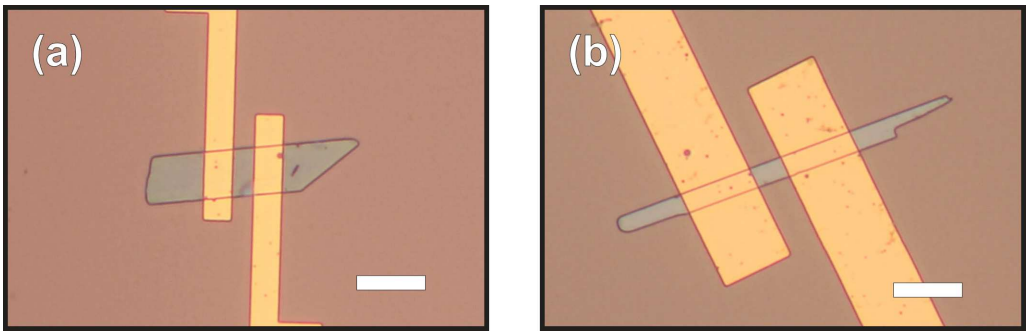

Figure 4.1: Optical images of two Hydrogen devices with contacts. The scale bar is 20 μm.

4.0.2 Current State of the Experiments

One of the issues with our method was using a copper holder with huge thermal capacity such that it was very hard to keep the system in a stable temperature. The copper holder acts as a giant heat sink so the time required for the temperature to be free of large hysterisis is too long and after the gases are

introduced to system the hysterisis would start again. As it can be seen from our results we haven't been able to collect reliable data yet. This study is yet to be finished, the chamber we are using seems to be not suitable for this kind of application.

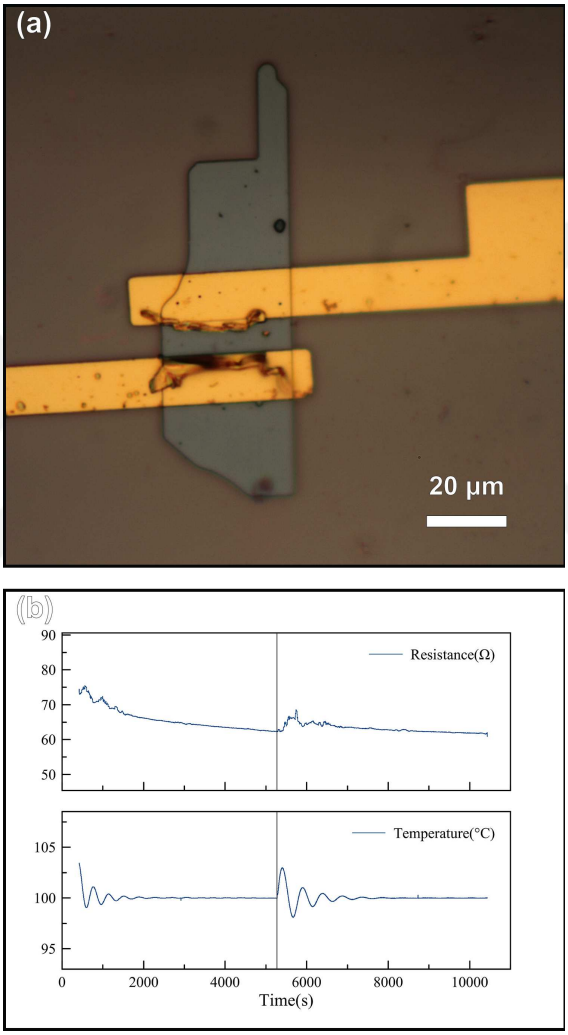

Figure 4.2: (a) shows a device made and measured for this project. Electrical Resistance Measurement of VO_2 while it is doped/undoped with H_2 gas (b). The vertical line shows the time where hydrogen flow is stopped. The device was first doped with a gas flow that is made up of 60 sccm Ar and 30 sccm H_2. Then the H_2 flow is stopped so that only 60 sccm Ar was given to system which makes VO_2 crytal release the hydrogen back to environment. The result of the doping shows that a drop in resistance at first which slows down but persists during both the doping and the undoping part. The fluctuation of the temperature is also visible.

Chapter 5

Conclusion and Future Work

In this thesis crystal growth of VO_2 is rigorously studied and applications made for TEM analysis and electronic property measurements. In Chapter-2, We have demonstrated a new method for VO_2 growth that can be used for TEM and hall bar studies. To best of our knowledge the single crystal VO_2 growth of low aspect ratio crystals with thickness between 75-170 nm and with the size of 50-100 μm is not known in the science community, this method can be a great use for device making and other scientific enquiries because of the better and easier handling it provides coming from its two dimensional morphology. Moreover we have showed that the chemical potency of Si/SiO_2, quartz and sapphire surfaces can be modified using only oxygen. With the new method provided in this thesis, the mechanics of VO_2 growth will be better understood and some important aspects of widely used growth substrates. Another important finding was a method for greatly increasing the yield of the CVD growth with the means of merely using the capabilities of the furnace. This represents a very basic idea to modify the nucleation properties of crystals. This method can be developed further to use more effectively via local heating of substrate or lasers so the growth can be more controlled.

Chapter-3 covers the TEM studies of Hydrogenated single crystal VO_2. We have not reached our goals completely on our TEM project, but the TEM analysis

of a single crystal H_xVO_2 O2 orthorombic structure was an interesting endevaour. Again to best of our knowledge this is the only TEM analysis of a single crystal VO_2 that is doped with Hydrogen on one half of the crystal while other side is pure VO_2. Our methods can be used to have a better understanding of the orthorombic phases of the H_xVO_2.

Finally we have made a two terminal device to understand the electronic aspect of Hydrogenation though the work is in its beginings. The resistance measurements in chapter-4 don't provide reliable data and it doesn't show a complete project. The set-up can be improved and more insight can be gained using the same idea.

By using the growth techniques we provided; experiments like Hall-Effect measurements can be performed on thin, single crystal VO_2 instead of thin poly crystalline films. This, we believe, will provide better results in terms of ease of conduct and reproducibility. Unlike the thin films, these crystals can be removed from the surface of substrate and transferred to ideal surfaces like hBN which would reduce the effects of stress on the electronic properties of the crystals. More exciting applications such as making Mott-Effect Transistors might be easier to be worked on using these crystals. Our method of Hydrogenation can be used to determine the orthorombic phase of Hydrogen doped VO_2 in a more controllable way, since the Hydrogenation can be better controlled and the resulting TEM samples doesn't need to be etched. Overall the techniques we have developed can be used in various applications, and they can provide better results and reproducibility for experiments while reducing the effort of manipulating the crystals for device making.

Bibliography

[1] S. Shin, S. Suga, M. Taniguchi, M. Fujisawa, H. Kanzaki, A. Fujimori, H. Daimon, Y. Ueda, K. Kosuge, and S. Kachi, "Vacuum-ultraviolet reflectance and photoemission study of the metal-insulator phase transitions in vo 2, v 6 o 13, and v 2 o 3," *Physical Review B*, vol. 41, no. 8, p. 4993, 1990.

[2] E. Strelcov, A. V. Davydov, U. Lanke, C. Watts, and A. Kolmakov, "In situ monitoring of the growth, intermediate phase transformations and templating of single crystal vo2 nanowires and nanoplatelets," *ACS Nano*, vol. 5, no. 4, pp. 3373–3384, 2011.

[3] G. Silversmit, D. Depla, H. Poelman, G. B. Marin, and R. De Gryse, "Determination of the V2p XPS binding energies for different vanadium oxidation states (V5+ to V0+)," *Journal of Electron Spectroscopy and Related Phenomena*, vol. 135, no. 2-3, pp. 167–175, 2004.

[4] J. Mendialdua, R. Casanova, and Y. Barbaux, "XPS studies of V2O5, V6O13, VO2 and V2O3," *Journal of Electron Spectroscopy and Related Phenomena*, vol. 71, no. 3, pp. 249–261, 1995.

[5] S. L. McArthur, "Thin films of Vanadium Oxide Grown on Vanadium metal," *Surface and Interface Analysis*, vol. 38, no. c, pp. 1380–1385, 2006.

[6] E. Morosan, D. Natelson, A. H. Nevidomskyy, and Q. Si, "Strongly correlated materials," *Advanced Materials*, vol. 24, no. 36, pp. 4896–4923, 2012.

[7] E. Dagotto, "R EVIEW Complexity in Strongly Correlated," *Science*, vol. 309, no. 5732, pp. 257–262, 2005.

[8] A. Cavalleri, T. Dekorsy, H. H. Chong, J. C. Kieffer, and R. W. Schoenlein, "Evidence for a structurally-driven insulator-to-metal transition in VO2: A view from the ultrafast timescale [2]," *Physical Review B - Condensed Matter and Materials Physics*, vol. 70, no. 16, pp. 1–4, 2004.

[9] M. Rini, A. Cavalleri, R. W. Schoenlein, R. López, L. C. Feldman, R. F. Haglund, L. A. Boatner, and T. E. Haynes, "Photoinduced phase transition in VO_2 nanocrystals: ultrafast control of surface-plasmon resonance," *Optics Letters*, vol. 30, no. 5, p. 558, 2005.

[10] S. Biermann, A. Poteryaev, A. I. Lichtenstein, and A. Georges, "Dynamical singlets and correlation-assisted peierls transition in vo 2," *Physical Review Letters*, vol. 94, no. 2, pp. 1–4, 2005.

[11] C. Blaauw, F. Leenhouts, F. Van Der Woude, and G. A. Sawatzky, "The metal-non-metal transition in VO2: X-ray photoemission and resistivity measurements," *Journal of Physics C: Solid State Physics*, vol. 8, no. 4, pp. 459–468, 1975.

[12] G. A. Sawatzky and D. Post, "X-ray photoelectron and Auger spectroscopy study of some vanadium oxides," *Physical Review B*, vol. 20, no. 4, pp. 1546–1555, 1979.

[13] J. B. Goodenough, "The two components of the crystallographic transition in VO2," *Journal of Solid State Chemistry*, vol. 3, no. 4, pp. 490–500, 1971.

[14] A. Srivastava, H. Rotella, S. Saha, B. Pal, G. Kalon, S. Mathew, M. Motapothula, M. Dykas, P. Yang, E. Okunishi, D. D. Sarma, and T. Venkatesan, "Selective growth of single phase VO2(A, B, and M) polymorph thin films," 2015.

[15] J. M. Atkin, S. Berweger, E. K. Chavez, M. B. Raschke, J. Cao, W. Fan, and J. Wu, "Strain and temperature dependence of the insulating phases of VO 2 near the metal-insulator transition," *Physical Review B - Condensed Matter and Materials Physics*, vol. 85, no. 2, pp. 1–4, 2012.

[16] J. I. Sohn, H. J. Joo, D. Ahn, H. H. Lee, A. E. Porter, K. Kim, D. J. Kang, and M. E. Wellandt, "Surface-stress-induced Mott transition and nature of associated spatial phase transition in single crystalline VO2 nanowires," *Nano Letters*, vol. 9, no. 10, pp. 3392–3397, 2009.

[17] A. Tselev, I. A. Luk'Yanchuk, I. N. Ivanov, J. D. Budai, J. Z. Tischler, E. Strelcov, A. Kolmakov, and S. V. Kalinin, "Symmetry relationship and strain-induced transitions between insulating M1 and M2 and metallic R phases of vanadium dioxide," *Nano Letters*, vol. 10, no. 11, pp. 4409–4416, 2010.

[18] H. Guo, K. Chen, Y. Oh, K. Wang, C. Dejoie, S. A. Syed Asif, O. L. Warren, Z. W. Shan, J. Wu, and A. M. Minor, "Mechanics and dynamics of the strain-induced M1-M2 structural phase transition in individual VO2 nanowires," *Nano Letters*, vol. 11, no. 8, pp. 3207–3213, 2011.

[19] J. L. Lebowitz, A. Martin-Lof, C. Math Phys, R. B. Griffiths, C. A. Hurst, S. Sherman, M. Marezio, D. B. Mc, J. P. Remeika, and P. D. Dernier, "MORE INEQUALITIES, FOR ISING FERROMAGNETS Structural Aspects of the Metal-Insulator Transitions in Cr-Doped," *J. Chem. Phys. Math. Phys*, vol. 12, no. 7, pp. 269–99, 1969.

[20] E. Strelcov, A. Tselev, I. Ivanov, J. D. Budai, J. Zhang, J. Z. Tischler, I. Kravchenko, S. V. Kalinin, and A. Kolmakov, "Doping-based stabilization of the M2 phase in free-standing VO2nanostructures at room temperature," *Nano Letters*, vol. 12, no. 12, pp. 6198–6205, 2012.

[21] K. D. Rogers, "An X-ray diffraction study of semiconductor and metallic vanadium dioxide," *Powder Diffraction*, vol. 8, no. 4, pp. 240–244, 1993.

[22] H. T. Kim, Y. W. Lee, B. J. Kim, B. G. Chae, S. J. Yun, K. Y. Kang, K. J. Han, K. J. Yee, and Y. S. Lim, "Monoclinic and correlated metal phase in VO2 as evidence of the mott transition: Coherent phonon analysis," *Physical Review Letters*, vol. 97, no. 26, pp. 10–13, 2006.

[23] M. S. Laad, L. Craco, and E. Müller-Hartmann, "Metal-insulator transition in rutile-based VO2," *Physical Review B - Condensed Matter and Materials Physics*, vol. 73, no. 19, pp. 1–7, 2006.

[24] M. W. Haverkort, Z. Hu, A. Tanaka, W. Reichelt, S. V. Streltsov, M. A. Korotin, V. I. Anisimov, H. H. Hsieh, H. J. Lin, C. T. Chen, D. I. Khomskii, and L. H. Tjeng, "Orbital-assisted metal-insulator transition in VO2," *Physical Review Letters*, vol. 95, no. 19, pp. 4–7, 2005.

[25] F. Gebhard, *Metal—Insulator Transitions*. Springer, 1997.

[26] N. Mott, "Metals, nonmetals and metal-nonmetal transitions: Some recollections," *Reports on Progress in Physics*, vol. 47, no. 8, pp. 909–923, 1984.

[27] N. Mott, "Metal-Insultaor Transition," *Reviews of Modern Physics*, vol. 40, no. 4, 1968.

[28] G. Stefanovich, A. Pergament, and D. Stefanovich, "Electrical switching and Mott transition in VO2," *Journal of Physics Condensed Matter*, vol. 12, no. 41, pp. 8837–8845, 2000.

[29] D. Ruzmetov, D. Heiman, B. B. Claflin, V. Narayanamurti, and S. Ramanathan, "Hall carrier density and magnetoresistance measurements in thin-film vanadium dioxide across the metal-insulator transition," *Physical Review B*, vol. 79, p. 153107, apr 2009.

[30] H. T. Kim, B. G. Chae, D. H. Youn, S. L. Maeng, G. Kim, K. Y. Kang, and Y. S. Lim, "Mechanism and observation of Mott transition in VO2-based two- and three-terminal devices," *New Journal of Physics*, vol. 6, 2004.

[31] W. Burkhardt, T. Christmann, S. Franke, W. Kriegseis, D. Meister, B. K. Meyer, W. Niessner, D. Schalch, and A. Scharmann, "Tungsten and fluorine co-doping of VO2films," *Thin Solid Films*, vol. 402, no. 1-2, pp. 226–231, 2002.

[32] A. Romanyuk, R. Steiner, L. Marot, and P. Oelhafen, "Temperature-induced metal-semiconductor transition in W-doped VO2films studied by

photoelectron spectroscopy," *Solar Energy Materials and Solar Cells*, vol. 91, no. 19, pp. 1831–1835, 2007.

[33] J. W. Byon, M. B. Kim, M. H. Kim, S. Y. Kim, S. H. Lee, B. C. Lee, and J. M. Baik, "Electrothermally induced highly responsive and highly selective vanadium oxide hydrogen sensor based on metal-insulator transition," *Journal of Physical Chemistry C*, vol. 116, no. 1, pp. 226–230, 2012.

[34] M. Rini, A. Cavalleri, R. W. Schoenlein, R. López, L. C. Feldman, R. F. Haglund, L. A. Boatner, and T. E. Haynes, "Photoinduced phase transition in vo 2 nanocrystals: ultrafast control of surface-plasmon resonance," *Optics letters*, vol. 30, no. 5, pp. 558–560, 2005.

[35] Y. Gao, H. Luo, C. Cao, X. Liu, Z. Chen, Z. Zhang, J. Zhou, and L. Dai, "VO2 thermochromic smart window for energy savings and generation," *Scientific Reports*, vol. 3, no. 1, pp. 1–5, 2013.

[36] E. Strelcov, Y. Lilach, and A. Kolmakov, "Gas Sensor Based on Metal-Insulator Transition in VO2 Nanowire Thermistor," *Nano Letters*, vol. 9, no. 6, pp. 2322–2326, 2009.

[37] J. Wei, H. Ji, W. Guo, A. H. Nevidomskyy, and D. Natelson, "Hydrogen stabilization of metallic vanadium dioxide in single-crystal nanobeams," *Nature Nanotechnology*, vol. 7, no. 6, pp. 357–362, 2012.

[38] B. Hu, Y. Ding, W. Chen, D. Kulkarni, Y. Shen, V. V. Tsukruk, and Z. L. Wang, "External-strain induced insulating phase transition in VO2nanobeam and its application as flexible strain sensor," *Advanced Materials*, vol. 22, no. 45, pp. 5134–5139, 2010.

[39] Y. Filinchuk, N. A. Tumanov, V. Ban, H. Ji, J. Wei, M. W. Swift, A. H. Nevidomskyy, and D. Natelson, "In situ diffraction study of catalytic hydrogenation of VO2: Stable phases and origins of metallicity," *Journal of the American Chemical Society*, vol. 136, no. 22, pp. 8100–8109, 2014.

[40] A. M. Chippindale, P. G. Dickens, and A. V. Powell, "Synthesis, characterization, and inelastic neutron scattering study of hydrogen insertion compounds of vo2(rutile)," *Journal of Solid State Chemistry*, vol. 93, no. 2, pp. 526–533, 1991.

[41] A. Schwartz, "the Promise of," *Science*, vol. 350, no. 6256, pp. 10–11, 2015.

[42] J. Wei, Z. Wang, W. Chen, and D. H. Cobden, "New aspects of the metal–insulator transition in single-domain vanadium dioxide nanobeams," *Nature Nanotechnology*, vol. 4, no. 7, pp. 420–424, 2009.

[43] W. H. Rosevear and W. Paul, "Hall Effect in V O 2 near the Semiconductor-to-Metal Transition," *Physical Review B*, vol. 7, pp. 2109–2111, mar 1973.

[44] B. S. Guiton, Q. Gu, A. L. Prieto, M. S. Gudiksen, and H. Park, "Single-crystalline vanadium dioxide nanowires with rectangular cross sections," *Journal of the American Chemical Society*, vol. 127, no. 2, pp. 498–499, 2005.

[45] C. Cheng, K. Liu, B. Xiang, J. Suh, and J. Wu, "Ultra-long, free-standing, single-crystalline vanadium dioxide micro/nanowires grown by simple thermal evaporation," *Applied Physics Letters*, vol. 100, no. 10, 2012.

[46] J. I. Sohn, H. J. Joo, A. E. Porter, C.-j. Choi, K. Kim, D. J. Kang, and M. E. Welland, "Direct Observation of the Structural Component of the Metal - Insulator Phase Transition and Growth Habits of Epitaxially Grown VO 2 Nanowires," *Nano Letters*, vol. 7, no. 6, pp. 1570–1574, 2007.

[47] M. R. Otto, L. P. R. de Cotret, D. A. Valverde-Chavez, K. L. Tiwari, N. Émond, M. Chaker, D. G. Cooke, and B. J. Siwick, "How optical excitation controls the structure and properties of vanadium dioxide," 2018.

[48] S. Y. Li, K. Namura, M. Suzuki, G. A. Niklasson, and C. G. Granqvist, "Thermochromic VO2 nanorods made by sputter deposition: Growth conditions and optical modeling," *Journal of Applied Physics*, vol. 114, no. 3, 2013.

[49] A. Hendaoui, N. Émond, M. Chaker, and É. Haddad, "Highly tunable-emittance radiator based on semiconductor-metal transition of VO2 thin films," *Applied Physics Letters*, vol. 102, no. 6, 2013.

[50] D. P. Zhang, M. D. Zhu, Y. Liu, K. Yang, G. X. Liang, Z. H. Zheng, X. M. Cai, and P. Fan, "High performance VO2 thin films growth by DC magnetron sputtering at low temperature for smart energy efficient window application," *Journal of Alloys and Compounds*, vol. 659, pp. 198–202, 2016.

[51] G. Garry, O. Durand, and A. Lordereau, "Structural, electrical and optical properties of pulsed laser deposited VO2 thin films on R- and C-sapphire planes," *Thin Solid Films*, vol. 453-454, pp. 427–430, 2004.

[52] K. Nagashima, T. Yanagida, H. Tanaka, and T. Kawai, "Influence of ambient atmosphere on metal-insulator transition of strained vanadium dioxide ultrathin films," *Journal of Applied Physics*, vol. 100, no. 6, pp. 1–5, 2006.

[53] H. Luo, Z. Chen, M. Kanehira, Z. Zhang, J. Du, C. Cao, Y. Gao, and L. Kang, "Nanoceramic VO2 thermochromic smart glass: A review on progress in solution processing," *Nano Energy*, vol. 1, no. 2, pp. 221–246, 2011.

[54] M. M. Seyfouri and R. Binions, "Sol-gel approaches to thermochromic vanadium dioxide coating for smart glazing application," *Solar Energy Materials and Solar Cells*, vol. 159, pp. 52–65, 2017.

[55] Y. F. Wu, L. L. Fan, S. M. Chen, S. Chen, C. W. Zou, and Z. Y. Wu, "Spectroscopic analysis of phase constitution of high quality VO2 thin film prepared by facile sol-gel method," *AIP Advances*, vol. 3, no. 4, 2013.

[56] B. S. Guiton, Q. Gu, A. L. Prieto, M. S. Gudiksen, and H. Park, "Single-crystalline vanadium dioxide nanowires with rectangular cross sections," *Journal of the American Chemical Society*, vol. 127, no. 2, pp. 498–499, 2005.

[57] J. M. Baik, M. H. Kim, C. Larson, A. M. Wodtke, and M. Moskovits, "Nanostructure-Dependent Metal - Insulator Transitions in Vanadium-Oxide Nanowires," pp. 13328–13331, 2008.

[58] H. Wriedt, "The ov (oxygen-vanadium) system," *Bulletin of Alloy Phase Diagrams*, vol. 10, no. 3, pp. 271–277, 1989.

[59] M. I. Vesselinov, *Crystal growth for beginners: fundamentals of nucleation, crystal growth and epitaxy*. World scientific, 2016.

[60] H. Leamy, G. Gilmer, and K. Jackson, "Statistical thermodynamics of clean surfaces," *Surface physics of materials*, vol. 1, p. 121, 1975.

[61] S. Yun and S. Ted Oyama, "Correlations in palladium membranes for hydrogen separation: A review," *Journal of Membrane Science*, vol. 375, no. 1-2, pp. 28–45, 2011.

[62] Y. Ebisuzaki, "Solubility and Diffusion of Hydrogen and Deuterium in Platinum," *The Journal of Chemical Physics*, vol. 49, no. 8, p. 3329, 1968.